
Theses and Dissertations

Summer 2008

The potential of cationic photopolymerization's long lived active centers

Beth Ann Ficek
University of Iowa

Follow this and additional works at: <https://ir.uiowa.edu/etd>

 Part of the [Chemical Engineering Commons](#)


Copyright 2008 Beth Ann Ficek

This dissertation is available at Iowa Research Online: <https://ir.uiowa.edu/etd/280>

Recommended Citation

Ficek, Beth Ann. "The potential of cationic photopolymerization's long lived active centers." PhD (Doctor of Philosophy) thesis, University of Iowa, 2008.
<https://doi.org/10.17077/etd.3qalv3px>

Follow this and additional works at: <https://ir.uiowa.edu/etd>

 Part of the [Chemical Engineering Commons](#)

THE POTENTIAL OF CATIONIC PHOTOPOLYMERIZATION'S LONG LIVED
ACTIVE CENTERS

by

Beth Ann Ficek

An Abstract

Of a thesis submitted in partial fulfillment of the
requirements for the Doctor of Philosophy degree
in Chemical and Biochemical Engineering in
the Graduate College of The University of Iowa

May 2008

Thesis Supervisor: Professor Alec B. Scranton

Photopolymerizations offer many advantages (such as temporal and spatial control of initiation, cost efficiency, and solvent-free systems) over traditional thermopolymerization. While they are now well-established as the preferred option for a variety of films and coating applications, they are limited from many applications due to problems such as oxygen inhibition, light attenuation, additive interference, and the creation of shadow regions and oxygen pockets due to complex shapes. These problems can be solved by using an underutilized form of photopolymerization--cationic photopolymerization.

Cationic photopolymerizations have unique active centers that are essentially non-terminating causing extremely long active center lifetimes. In this contribution, the unique characteristics of cationic active centers are explored for their use in many new applications where previous photopolymerization techniques failed. It was found that the long lifetimes of the active centers permitted them to be very mobile, allowing them to migrate into and polymerize regions that were never illuminated in a process termed shadow cure. The mobility of cationic active centers provides a very efficient means of photopolymerizing of thick and pigmented systems. The long lifetimes of the cationic active centers can be used in the creation of a sequential stage curable polymer system and in the development of novel methods to cure complex shapes, two applications previously unattainable by photopolymerization. The termination of the cationic active centers was found to be reversible and can be used as a technique for external temporal control of the photopolymerization after the illumination has ceased. These abilities have great potential and will allow cationic photopolymerization to be used in many new

applications where previous photopolymerization techniques failed, expanding their influence and benefits.

Abstract Approved: _____

Thesis Supervisor

Title and Department

Date

THE POTENTIAL OF CATIONIC PHOTOPOLYMERIZATION'S LONG LIVED
ACTIVE CENTERS

by

Beth Ann Ficek

A thesis submitted in partial fulfillment of the
requirements for the Doctor of Philosophy degree
in Chemical and Biochemical Engineering in
the Graduate College of The University of Iowa

May 2008

Thesis Supervisor: Professor Alec B. Scranton

Graduate College
The University of Iowa
Iowa City, Iowa

CERTIFICATE OF APPROVAL

PH.D. THESIS

This is to certify that the Ph.D. thesis of

Beth Ann Ficek

has been approved by the Examining Committee for the thesis requirement for the Doctor of Philosophy degree in Chemical and Biochemical Engineering at the May 2008 graduation.

Thesis Committee: _____
Alec B. Scranton, Thesis Supervisor

Julie L. P. Jessop

C. Allan Guymon

David Rethwisch

Johna Leddy

To God, Mom, and Dad, who made all things possible for me.

ACKNOWLEDGEMENTS

This research, like my life, was shaped by many people. While I would like to thank them all by name and contribution, doing so would double the length of this dissertation. I would like to express my sincere appreciation to a few who have been most influential. I would like to begin by giving my thanks to my advisor Dr. Alec Scranton, whose enthusiastic seminar talk back when I was a sophomore undergraduate introduced the wonderful world of photopolymerization to me. His guidance over my undergraduate and graduate years has been invaluable to me. I would also like to thank my professors who have taught me valuable lessons both through class work and as living examples. A special thanks to Dr. Allan Guymon, Dr. Julie Jessop, Dr. Johna Leddy, and Dr. David Rethwisch who served on my committee. I would also like to acknowledge Linda Wheatley, whose resources and knowledge of the inner university workings proved priceless over the years.

I am also grateful to my research group members both past and present, who became my friends and helped me through the day-to-day trials of research. My heartfelt thanks go to all of my undergraduate assistants--especially Amber Thiesen--whose hard work and dedication were immensely helpful in completing this research.

I am indebted to the many excellent industrial companies I have worked with over the years. This research was made possible by their funding and made better by their suggestions. My thanks includes the individual representatives of these companies who mentored me over the years, preparing me for the next stage in my career. In addition, I am would like to acknowledge the funding support in the form of a graduate fellowship from the National Science Foundation.

My thanks to Zack Rundlett, who has come into my life and made these past few years wonderful, and to Robyn Davis ,who befriended me in the first days of college and has been there for me every since.

Finally, I would like to express my thanks to my family who have inspired me throughout my life. I could not ask for a better support group. Whether it was deciphering my writing, translating it into a readable form, helping me with the hard decisions, or always being there to get away and have some fun, you made this work possible. Nana, Mom, Dad, Bonnie, Becky, Brother, and especially my best friend, the wee one, Brandy; I love you all and can't thank you enough.

TABLE OF CONTENTS

LIST OF TABLES	viii
LIST OF FIGURES	ix
CHAPTER 1. MOTIVATION AND BACKGROUND	1
1.1. Introduction.....	1
1.2. Photopolymerization Background	1
1.3. Photopolymerization Issues and the Current State of Technology	3
1.3.1. Oxygen Inhibition	3
1.3.2. Light Attenuation	4
1.3.3. Additive Interference	5
1.3.4. Complex Shapes.....	6
1.3.5. Control over Physical Property Changes	7
1.4. Cationic Photopolymerization: The Solution to Current Limitations	8
1.4.1. Overview of Cationic Properties.....	8
1.4.2. Mechanism/Kinetics	10
1.4.3. History of Cationic Photopolymerization	14
CHAPTER 2. OBJECTIVES.....	18
CHAPTER 3. ABILITY OF CATIONIC PHOTOPOLYMERIZATIONS TO CURE THICK SYSTEMS THROUGH ACTIVE CENTER MIGRATION	19
3.1. Introduction.....	19
3.2. Modeling the Spatial Profile of Active Centers Production	19
3.2.1. Governing Differential Equations.....	20
3.2.2. Modeling a Standard Cationic Photoinitiator/Monomer System.....	23
3.3. Active Center Mobility through Thick Polymer Systems.....	28
3.3.1. Active Center Migration Experiments	28
3.3.1.1. Materials	28
3.3.1.2. Photopolymerization	29
3.3.1.3. Characterization of Shadow Cure	29
3.3.2. Active Center Migration Results and Discussion	30
3.3.2.1. Time Dependence of Shadow Cure	30
3.3.2.2. Effect of Temperature	34
3.3.2.3. Effect of the Photoinitiator Counter-ion	35
3.3.2.4. Effect of Photoinitiator Concentration.....	37
3.3.2.5. Effect of Exposure Time	38
3.4. Modeling Active Center Mobility through Thick Polymer Systems	39
3.4.1. Active Center Migration Model.....	40

3.4.2. Verification of the Active Center Migration Model	41
3.5. Conclusions.....	43
CHAPTER 4: ABILITY OF CATIONIC PHOTOPOLYMERIZATIONS TO CURE PIGMENTED SYSTEMS	45
4.1. Introduction.....	45
4.2. Research Method	45
4.2.1. Materials	45
4.2.2. Experimentation Method	46
4.3. Research Results Using Carbon Black	47
4.3.1. Effect of Carbon Black Loading.....	49
4.3.2. Effect of Temperature	50
4.3.3. Effect of Exposure Time.....	51
4.4. Experimental Results using Titanium Dioxide.....	51
4.5. Research Results using Other Additives.....	53
4.5.1. UV Absorbers	54
4.5.2. Hindered Amine Light Stabilizer.....	55
4.6. Conclusions.....	56
CHAPTER 5: ABILITY OF CATIONIC PHOTOPOLYMERIZATIONS TO CURE COMPLEX SHAPES	58
5.1. Introduction.....	58
5.2. Research Method	60
5.2.1. Materials	60
5.2.2. Methods.....	61
5.3. Results and Discussion	61
5.3.1. Effect of Storage Time on Active Centers Produced in Monomer-free Solution.....	61
5.3.2. Effect of Storage Temperature on Active Centers Produced in Monomer-free Solution	63
5.4. Conclusions.....	63
CHAPTER 6: CREATING SEQUENTIAL STAGE CURABLE POLYMERS WITH CATIONIC PHOTOPOLYMERIZATIONS.....	65
6.1. Introduction.....	65
6.2. Background of Sequential Stage Curable Hybrid Systems.....	66
6.3. Research Methods.....	68
6.4. Research Results	69
6.4.1. Control of Sequential Stage Curable Hybrid Systems through Monomer Selection	69
6.4.2. Control of Sequential Stages through Free Radical/Iodonium Salt Photoinitiation System.....	75
6.5. Conclusions.....	78

CHAPTER 7: ABILITY OF CATIONIC PHOTOPOLYMERIZATIONS TO ACHIEVE TEMPORAL CONTROL OF POLYMERIZATION THROUGH A REVERSIBLE WATER INHIBITION	79
7.1. Introduction.....	79
7.2. Background on Cationic Photopolymerization Water Sensitivity	79
7.3. Research Methods.....	81
7.3.1. Materials	81
7.3.2. Methods.....	82
7.4. Results and Discussion	83
7.4.1. Effect of Moisture Concentration: Water Inhibition.....	83
7.4.2. Varying Moisture Concentration in Situ: Reversing the Water Inhibiton	84
7.5. Conclusion	86
CHAPTER 8: CONCLUSIONS AND RECOMMENDATIONS	88
8.1. Cationic Photopolymerization’s Ability to Cure Thick Systems through Active Center Migration.....	88
8.2. Cationic Photopolymerization’s Ability to Cure Pigmented Systems	89
8.3. Cationic Photopolymerization’s Ability to Cure Complex Shapes	90
8.4. Creating Sequential Stage Curable Polymers with Cationic Photopolymerizations	91
8.5. Cationic Photopolymerizations Ability to Achieve Temporal Control of Polymerization Through a Reversible Water Inhibition.....	92
REFERENCES	93

LIST OF TABLES

Table 4.1. Time to achieve tack-free cure for systems with 0-6wt% CB pigment loadings.	50
Table 4.2. Time to achieve tack-free cure for 3wt% CB polymer systems illuminated for different durations.	51
Table 4.3. Time to achieve tack-free cure for systems with 0-6wt% TiO ₂ pigment loadings.	52
Table 4.4. Time to achieve tack-free cure for 3wt% TiO ₂ polymer systems illuminated for different durations.	53
Table 6.1. Comparison of different photoinitiation systems used in the polymerization of a 20% monoacrylate / 80% diepoxide hybrid monomer solution.....	77
Table 7.1. Induction time and time to reach 50% conversion for cationic photopolymerizations in nitrogen atmospheres of 0%, 50%, and 100% relative saturation.....	84

LIST OF FIGURES

Figure 1.1. Example of direct cationic photo-initiation mechanism.....	10
Figure 1.2. Example of in-direct cationic photo-initiation mechanism	12
Figure 1.3. Example of cationic propagation mechanism.....	13
Figure 1.4. Example of cationic termination by counter-ion combination mechanism.....	14
Figure 3.1. Molecular structure of 3,4-epoxycyclohexylmethanyl 3,4- epoxycyclohexanecarboxylate.	23
Figure 3.2. Molecular structure of (tolycumyl) iodonium tetrakis (pentafluorophenyl) borate.....	23
Figure 3.3. Spectra for the Hg-Xe arc lamp emission and the photoinitiator IPB absorbance.	24
Figure 3.4. Evolution of profiles during illumination for: A) the total light intensity summed over the initiating wavelengths (295-307 nm) and B) the photoinitiator concentration.	26
Figure 3.5. Evolution of active center rate production profiles during illumination.	27
Figure 3.6. Evolution of the active center concentration profiles during illumination.	28
Figure 3.7. Molecular structure of diaryliodonium hexafluoroantimonate.....	29
Figure 3.8. Proof of shadow cure; sample heights over time with no additional illumination.	31
Figure 3.9. Shadow cure dependence on time: A) linear time axis and B) square root time axis.	33
Figure 3.10. Effect of temperature on shadow cure.....	34
Figure 3.11. Arrhenius relationship between temperature and effective diffusion coefficient.....	35
Figure 3.12. Active center concentration profiles of photoinitiators with different counter-ions.	36
Figure 3.13. Effect of photoinitiator counter-ion on shadow cure.....	36

Figure 3.14. Active center concentration profiles of different photoinitiators concentrations.....	37
Figure 3.15. Effect of photoinitiator concentration on shadow cure.	38
Figure 3.16. Effect of the exposure time on shadow cure.	39
Figure 3.17. Modeled active center spatial profiles during shadow cure.	41
Figure 3.18. Predicted and experimental polymer height for a thick system.	42
Figure 3.19. Predicted and experimental polymer height for a thick system.	42
Figure 4.1. Active center concentration profiles modeling effect of carbon black....	47
Figure 4.2. A thick 1wt% carbon black polymer created by shadow cure.	48
Figure 4.3. Active center concentration profiles for carbon black with different pigment loadings.	49
Figure 4.4. Active center concentration profiles modeling effect of TiO ₂ as compared to CB and neat systems.....	52
Figure 4.5. Active center concentration profiles modeling effect of UVA in comparison to other additives.	54
Figure 4.6. Active center concentration profiles modeling effect of HALS in comparison to other additives.	56
Figure 5.1. Method for using previously generated active centers in two step process.....	59
Figure 5.2. Method for using previously generated active centers in single step process.....	59
Figure 5.3. Molecular structure of triarylsulfonium hexafluoroantimonate salts (THA).	60
Figure 5.4. Molecular structure of methyl 3,4-epoxycyclohexanecarboxylate.	60
Figure 5.5. Polymerization rate profiles produced using previously photogenerated cationic active centers for two different storage times.	62
Figure 5.6. Normalized maximum rate of polymerization by previously photogenerated cationic active centers over storage time.	62

Figure 5.7. Normalized maximum rate of polymerization by previously generate cationic active centers dependence on storage time for two different temperatures.	63
Figure 6.1. The development of the sequential stages in a free radical/cationic hybrid system.	66
Figure 6.2. Typical photopolymerization induction times for several monomers.	70
Figure 6.3. Heat profiles comparing the 20% acrylate / 80% epoxide hybrid photopolymerization to neat acrylate and epoxide photopolymerizations.	71
Figure 6.4. Normalized heat profiles comparing the 20% acrylate / 80% epoxide hybrid photopolymerization to neat acrylate and epoxide photopolymerizations.	72
Figure 6.5. Rate of polymerization profiles comparing the 20% acrylate / 80% epoxide hybrid photopolymerization to neat acrylate and epoxide photopolymerizations.	73
Figure 6.6. Rate profiles showing the effect of epoxide/acrylate ratios has on the photopolymerizations and therefore the sequential stages of the hybrid system.	75
Figure 6.7. Cycloaliphatic epoxide induction times showing the effect that the percent of cycloaliphatic epoxide in the monomer system has on hybrid photopolymerization kinetics.	75
Figure 6.8. Initiation scheme of free radical initiator/iodonium salt hybrid photoinitiators.	76
Figure 7.1. Reactions of water and cationic active centers in vinyl ether polymerization systems without hydroxyl end groups.	81
Figure 7.2. Molecular structure of dodecyl vinyl ether (DVE).	81
Figure 7.3. Molecular structure of iodonium triflate salt (IT)	82
Figure 7.4. Conversion versus time for cationic photopolymerizations of DVE in nitrogen atmospheres of 0%, 50%, and 100% relative saturation.	84
Figure 7.5. Monomer conversion vs. time for DVE under fully saturated nitrogen atmosphere which is switched to dry nitrogen atmospheric conditions after 25 minutes.	86

Figure 7.6. Monomer conversion of DVE vs. time immediately after a fully saturated nitrogen atmosphere is switched to dry nitrogen atmospheric conditions at 25 minutes. 86

CHAPTER 1. MOTIVATION AND BACKGROUND

1.1. Introduction

Photopolymerizations is a rapidly growing multi-billion-dollar industry. One cause of this growth is that photopolymerizations are a more environmentally friendly system than the traditional polymerizations. Photopolymerizations achieve high production rates without the use of volatile organic compounds, which cause many adverse environmental and health effects and are becoming more restricted each year.¹ In addition, photopolymerizations have tremendous energy savings over thermal polymerizations by eliminating solvent handling systems and high temperature ovens. It has been estimated that energy costs can be cut 20-25% by switching from thermal polymerization to photopolymerization.² Clear coats, dental composites, microelectronics, and inks are just a few of the fields in which this exceptional polymerization process is being used.³ However, there are a number of problems in applying photopolymerization due to oxygen inhibition, light attenuation, additive interference, or the creation of shadow regions and oxygen pockets due to complex shapes.

These problems can be solved by using an underutilized form of photopolymerization-- cationic photopolymerization. Cationic photopolymerizations' unique active centers give them the ability to cure in atmosphere (with no oxygen inhibition), in the dark (in regions previously illuminated after the exposure has ceased) and even in shadow regions (regions that have had no illumination). These abilities have great potential and will allow cationic photopolymerization to be used in many new applications where previous photopolymerization techniques failed.

1.2. Photopolymerization Background

Since the invention of synthetic (man-made) plastics in 1909, plastics seem to have taken over the world. People's cars, furniture, electronics, clothes, even their medicines are plastic or

contain plastic parts. Plastics are made up of long chains of repeating molecules. These molecules are referred to as “mers” or monomers (unlinked single molecules) and since plastics are made up of these chains, which can be thousands of molecules long, they are known as polymers (many linked molecules). The process of linking them together is known as polymerization (or cure) and has three steps. The first step of polymerization is known as initiation. The polymer chain begins with a special chemical molecule called an initiator. When the initiator absorbs energy it reacts and changes into a molecule with an active center. The active center typically is either a free radical (the most common type of active center) or a cation. Either type of active center will then find a monomer, link it to the chain, and move to the end of the chain. The active center will repeat this process of finding unreacted monomers and linking them to the chain thousands of times in the second step of polymerization, known as propagation. To end the polymerization and complete the plastic, a reaction will happen to stop the active center from continuing to link up the monomers. This is the final step known as termination.

Polymers are typically divided into categories by the first step in the polymerization process, the initiation. If the energy the initiator absorbs is heat then it is known as thermal polymerization. Thermal polymerization is the most widely used mode of generating active centers in both industrial and academic settings. Thermal polymerization initiators usually include compounds with an O-O, S-S, or N-O bond, with peroxides typically being the most widely used.⁴ Thermal polymerization has a number of disadvantages. One disadvantage is the large amount of energy needed to raise the entire coating or part to a high temperature. A second disadvantage is many substrates, such as printed circuit boards, paper or wood, that require polymer coatings are very sensitive to heat and will degrade under elevated temperatures.⁵

The energy absorbed by the initiator to produce the active center does not have to be heat. It has been found that the certain wavelengths of light can also be absorbed and used to produce active centers. This type of polymerization is known as photopolymerization. Photopolymerization has many advantages over more traditional polymerizations. There is a low capital cost associated with this process. The cost of lamps and the energy required to operate the lamps is very low. Photopolymerizations are also more environmentally friendly. Polymerization traditionally used harmful volatile solvents (VOCs) as coalescing agents, to keep the binder soft and available to form a film as the solvent evaporates. Photopolymerization eliminates this need since the film is formed upon illumination so the monomer formulation is either high or 100% solids.⁵ Furthermore the low energy consumption also saves energy, lowering the emission of pollutants from power plants. Another benefit of using photopolymerization is the rapid cure time and high productivity at room temperature associated with the process when compared to thermal polymerizations.¹ Despite these advantages, photopolymerizations have not been able to work in all fields due to several issues.

1.3. Photopolymerization Issues and the Current State of Technology

1.3.1. Oxygen Inhibition

One of the largest problems facing the photopolymerization industry is the inhibition of polymerization by oxygen. Oxygen will react with any free radical active center halting the polymerization until all of the oxygen is consumed. This reaction creates peroxide and hydroperoxide by-products that are detrimental to the system. Oxygen inhibition leads to a number of problems including: incomplete polymerization, slow reaction rates, and tacky surfaces. A number of methods are used to overcome this problem. Blanketing a system with an inert gas such as nitrogen (eliminating oxygen from the system) is a typical industrial process.¹

However, this process requires large expensive inerting chambers and is usually not completely efficient due to the oxygen pockets remaining in complex shapes. Several other methods include addition of oxygen scavengers to eliminate the oxygen, use of higher photoinitiator concentration or higher intensity to produce more radicals to react with both the oxygen and monomer, and the use of shielding films to eliminate oxygen from dissolving into the monomer film.^{1,6} Since only free radicals are affected by the oxygen, different photopolymer systems, such as cationic^{1,5} or hybrid cationic/free radical⁷⁻¹³ (where the cationic active centers polymerize the monomer) can be used to avoid oxygen inhibition.

1.3.2. Light Attenuation

Light attenuation in larger sample depths has caused photopolymerization to be relatively unemployable in thick polymer applications (greater than 1 cm). Light attenuation is where the intensity of the light falls off as it is absorbed by the photoinitiator.¹ This means the photons being absorbed by the photoinitiators closer to the illumination source reduce the number of photons that can reach the photoinitiators located in the deeper regions of the sample. This leads to non-uniform and incomplete cures specifically in the deeper regions of the samples.

Currently, there are several methods which have been proposed to circumvent this problem. These methods have mostly focused on free radicals even though light attenuation is a problem for both free radical and cationic photopolymerization. One method is to bombard the sample with photons in the hopes that some will get through to the deeper regions of the samples. While this process works, it leads to expensive high intensity lamps and property gradients from the uneven cure. By lowering the initiator concentration, thicker polymer samples can be produced (since there is less initiator to absorb the photons at the surface) but their thickness is limited.¹ Recently, it has been reported that with the careful selection of photobleaching

initiators, thick polymer samples can be created with photopolymerization.^{14,15,16} While this method is very good for the polymerizing thick systems, its resulting non-uniform initiation rate profile is very complex and hard to navigate. Another method used to polymerize thick systems is dual cure or hybrid photo/thermal polymerization, where the sample first undergoes a typical photopolymerization polymerizing the illumination surface of the thick polymer, followed by a thermal polymerization which reacts the deeper shadow regions of the sample.⁵ This heat needed for the thermal cure can be applied externally using an oven (which eliminates one of the major cost-saving advantages of photopolymerization) or internally using the heat generated by the photopolymerization reaction (such as thiol-enes). Dual cure still has problems associated with it. Using an external heat source to produce the dual cure, defeats one of the main goals of photopolymerization, removing the heat source. If the heat is generated by an exothermic reaction, there is a limited selection of monomers that are exothermic enough to raise the sample temperature enough so the thermal polymerization can occur. This limits the range of the polymer properties reducing their versatility.

1.3.3. Additive Interference

Light attenuation can also be a problem for thin film photopolymerization systems with the addition of additives. Additives (typically pigments or fillers) can absorb or reflect the incoming photons which the photoinitiators need to react, hindering light-induced active center formation especially beneath the surface. This causes incomplete cures of pigmented systems and uneven cures resulting in wrinkling of the surface, problems which eliminate photopolymerizations as a possibility in these systems.¹ These additives are necessary for many applications and represent a large market in which photopolymerization has been unable to break into. Strategies for avoiding this additive interference with the photopolymerization include

trying to match photoinitiators and additives that absorb different wavelengths.² This is not possible for many applications because the additive either absorbs all wavelengths (like carbon black or UV stabilizers) competing with the photoinitiators for the photons, or reflects all the wavelengths (like titanium dioxide) preventing photons from entering the system. This interference leads to incomplete cures on all but the thinnest films (1-2 μ m).¹ Few methods have been developed to circumvent this problem. Using higher photoinitiator concentrations and light intensities can increase the probability of a photoinitiator absorbing the photon rather than an additive. However, that leads to higher costs since the photoinitiators and light sources are expensive and the concentrations and intensities still might not be enough to overcome the additive interference. The dual cure use for polymerization of thick systems can also be applied to pigmented systems but the deficiencies previously discussed still apply.

1.3.4. Complex Shapes

Photopolymerization is well established in a number of coating applications including paper, furniture and vinyl flooring. These applications are predominately coatings on flat, geometrically simple and symmetrical substrates. One of the largest challenges of photopolymerization is the inability to attain full polymerization on complex, three dimensional shapes. With complex shapes, some regions may be shaded from the initiating light source, and it is important that these “shadow regions” cure to a tack-free state. In addition, oxygen (which often inhibits polymerization) is very hard to remove from a complex system since it may remain trapped in pockets where there is little gas flow.

To prevent these shadow regions from occurring, many complicated lighting schemes have been devised. One scheme is to robotically rotate the three dimensional parts so every angle and every region is exposed.¹⁷ This method cannot not be used effectively with very large

substrates (such as automotive bodies) since the large objects are difficult to maneuver in confined spaces. A second scheme is to move the complex substrate through a tunnel of lights carefully set to maintain a uniform exposure on the entire objects.¹⁷ The scheme also has its disadvantages. The first is that the lamps must be carefully aligned through rigorous trial and error iterations or complex computer simulations to maintain the uniform illumination. A second disadvantage is the large capital cost associated with maintaining several lamps each with its own power supply and controller. With the development of robotics, a third scheme to photopolymerize complex shapes has emerged. In this scheme, the initiating light is placed on a mobile robotic arm which rotates and traverses around the complex coated object. This method has had varying degrees of success, but devising the path the robotic light needs to take is very intricate and shadow regions can easily occur with any miscalculation or misalignment.¹⁷

1.3.5. Control over Physical Property Changes

Photopolymerizations do not have much temporal control of their physical properties. Since the photopolymerization happens very quickly in comparison to thermal polymerizations, the sample physical properties are generally in two states: its unreacted liquid monomer form or in its final solid polymerized form. Control over these two stages is established by the timing of the illumination (before illumination, liquid; after illumination, solid). There are many application where using light to control the physical property change is not possible. One such field is adhesives. In adhesives, only when the monomer is sandwiched between two substrates is it desirable for it to be turned into polymer. If both substrates are opaque, then the light cannot reach the photoinitiator to create the active centers and photopolymerization is impossible. These adhesives must currently be made using solvents (VOCs) that evaporate or by thermopolymerization. Each of these methods has inherent problems. A process where the

active centers are generated through illumination but has another factor temporally controlling their polymerization of the monomer is desirable.

Photopolymerization where the physical properties go through more than two physical states is also desirable for many applications including; medical systems, rapid prototyping resins, advanced coatings and adhesives. For example, the transition from a low viscosity liquid, to a moldable putty, and finally to a hard, rigid polymer is attractive for dental restorations. The initial low viscosity state would allow the resin to readily fill the small holes and spaces in the teeth while the second stage would allow the mixture to be readily molded and shaped by the dentist before the resin assumes the final rigid state.

Temporal control over these stages is usually obtained by having two independent initiators that are activated by distinct wavelengths of light. By switching the irradiation source or removing a filter, each polymerization may be initiated in the desired order or time.³ Again, this type of temporal control through multiple lighting schemes is not desirable in many applications. For example, in a repositionable sealant or adhesive it is necessary for the system in a tacky stage, which allows the substrate to be moved around and adjusted, to enter its final rigid stage without having to remove it from the substrate to re-illuminate the adhesive. Having temporal control over the stages without having two illumination schemes would be beneficial in many other applications where minor adjustments need to be made before the final rigid polymer is needed.

1.4. Cationic Photopolymerization: The Solution to Current Limitations

1.4.1. Overview of Cationic Properties

Cationic photopolymerization are light-induced chemical reactions where cationic active centers propagate through monomer forming long polymer chains. The mechanics of this

reaction will be discussed more thoroughly in the next section. The unique properties of cationic active centers give cationic photopolymerizations several distinct advantages compared to the more common free radical photopolymerization. Foremost, the cationic active centers do not react with oxygen, allowing them to be used in atmospheric conditions. The cationic active centers do not have rapid the radical-radical termination reaction that free radical photopolymerization has and as a result of this non-terminating nature, the cationic active centers have extremely long lifetimes.^{3,18} These long lifetimes cause the reaction to proceed long after the irradiation has ceased, consuming nearly all of the monomer (a process known as dark cure).⁵ Furthermore, the lifetimes are long enough that slow driving forces like diffusion may affect the process. These driving forces will propel the active centers into unexposed regions (a process that will be termed shadow cure) breaking the first rule of photopolymerization--polymerization only happens where the illumination has occurred. The ability to dark and shadow cure has tremendous potential in solving many problems in the photopolymerization field.

The cationic active centers allow the polymerization of very important classes of monomers, including oxiranes (epoxides), oxetanes, siloxanes, and vinyl ethers. Furthermore, the cured polymer films associated with these monomers exhibit excellent clarity, adhesion, abrasion resistance, and chemical resistance. In addition, the cationic ring-opening photopolymerizations exhibit less shrinkage than free radical photopolymerizations of unsaturated monomers such as acrylates and methacrylates.

Despite these advantages, cationic photopolymerization is not a perfect system. One disadvantage of cationic photopolymerization is that water may inhibit the polymerization. Also, ring-opening cationic photopolymerizations generally exhibit slower polymerization rates compared to free radical photopolymerizations. Even with these disadvantages, cationic

photopolymerization has a great potential toward solving many of the major problems plaguing current photopolymerization techniques.

1.4.2. Mechanism/Kinetics

Cationic polymerizations begin with the initiation step (the photochemical reaction in which active centers are produced); then proceed to the propagation step in which the active center reacts successively with a number of monomer molecules to link them covalently into a polymer chain. The photoinitiation step is the only step that is dependent on light, and once the active centers are produced, they propagate without any further interaction with light. The photoinitiation's reaction mechanism depends on the structure of photoinitiator being used. The most common and effective cationic photoinitiators are diaryl-iodonium and triaryl-sulfonium salts. The diaryliodonium and triarylsulfonium salts can generate active centers through either direct excitation (absorption of the light leading to photolysis) or indirect excitation (where a photosensitizer absorbs the light and through several reactions the initiator is photolyzed). An example of a common direct photoinitiation reaction mechanism is shown in Figure 1.1. In direct photoinitiation the iodonium salt absorbs the photons and breaks apart (photolysis) in a primary unimolecular bond cleavage forming both cationic active centers and a non-reacting free radical active centers.¹

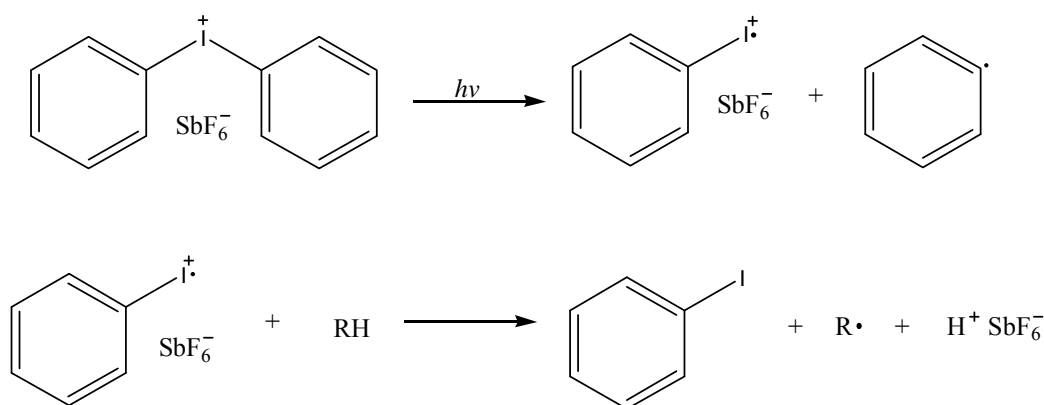


Figure 1.1. Example of direct cationic photo-initiation mechanism.

An example of a common indirect photoinitiation reaction mechanism is shown in Figure 1.2. This three-component initiator systems generally contains a light absorbing photosensitizer (sensitizers, dyes, or camphorquinone in this example), an electron donor (typically an amine which cannot be too basic else it will interfere with the propagation), and a third component (often a diaryliodonium or sulfonium salt).¹⁹ In this process the photosensitizer absorbs the light and becomes excited. Then it undergoes an electron transfer with the electron donor. The electron transfer must be thermodynamically feasible for the photoinitiation to occur. The Rhem-Weller equation, equation 1.1, is used to characterize the feasibility of this electron transfer.²⁰

$$\Delta G_{et} = F[E_{ox}(D/D^{\cdot+}) - E_{red}(A/A^{\cdot-})] - E^* \quad (1.1)$$

where ΔG_{et} is the change in Gibbs free energy for the electron transfer, which must be negative for electron transfer to be thermodynamically favored; F is Faraday's constant; $E_{ox}(D/D^{\cdot+})$ is the oxidation potential of the electron donor; $E_{red}(A/A^{\cdot-})$ is the reduction potential for the photosensitizer; E^* is the excited state energy of the electron acceptor. Once the electron transfer occurs, the electron deficient electron donor will undergo a proton transfer and emit the cationic active center. The use of this indirect photoinitiation allows a large variety of wavelengths (including several in the visible light region) to initiate a cationic photopolymerization.²¹

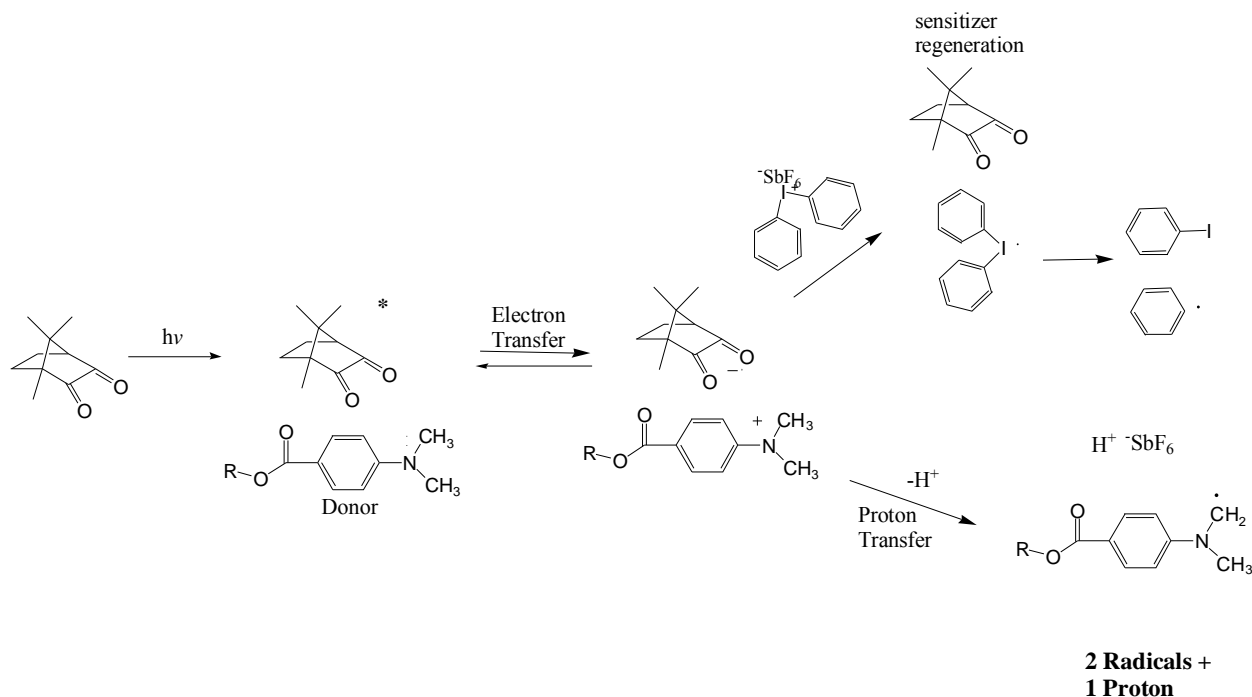


Figure 1.2. Example of in-direct cationic photo-initiation mechanism²¹

Once the cationic active centers are generated, they will begin to propagate through the monomers polymerizing the system. The generally accepted propagation mechanism for the cationic ring-opening polymerization of an epoxide (ethylene oxide in this case) is shown in Figure 1.3. According to this mechanism, the proton of the superacid (the cation, H^+ with the hexafluoroantimonate counterion) undergoes an electrophilic addition to the oxygen atom present in the epoxide ring, resulting in the formation of an oxonium ion, which is the propagating species.¹ The α -carbon of the oxonium ion is electron deficient due to its proximity to the positively charged oxygen, and is therefore subject to nucleophilic attack by a monomer unit. This nucleophilic attack opens the epoxide ring (by breaking the carbon-oxygen bond) and produces a new oxonium ion, thereby propagating the active center to the new monomer unit. This process is repeated a number of times to make a polymer chain, and the polymer chain

length is determined by the number of propagation steps that occur before the active center undergoes chain transfer or termination.

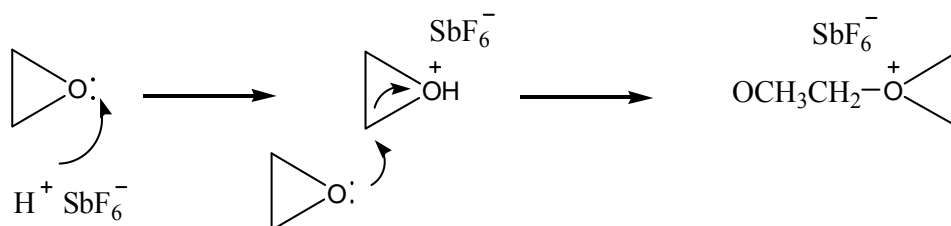


Figure 1.3. Example of cationic propagation mechanism.

Cationic photopolymerization has very low amounts of chain termination. The most common is a chain transfer where, in the presence of a Lewis base such as alcohols or polyols, a growing cationic polymer chain may undergo a chain transfer reaction which results in the termination of one growing chain and the generation of a proton capable of initiating a new chain.⁵ This reaction can have a significant effect on the structure of the polymer, especially in crosslinked systems. Combination with a counter-ion, shown in Figure 1.4, is another possible termination reaction. The counter-ion is present in the system due to the photoinitiator and allows the possibility of termination but the reaction is unlikely. Therefore, cationic photopolymerizations are considered essentially non-terminating in contrast to the free radical light-induced polymerizations which experience a rapid radical-radical termination reaction.^{3,5,18} As a consequence of the non-terminating nature, the cationic active centers have extremely long lifetimes, and cause the reaction to proceed long after the irradiation has ceased, consuming nearly all of the monomer (a process known as dark cure or post-polymerization).²²

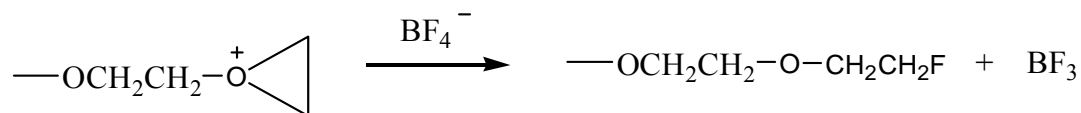


Figure 1.4. Example of cationic termination by counter-ion combination mechanism.

1.4.3. History of Cationic Photopolymerization

Despite having several superior advantages over free radical photopolymerization, cationic photopolymerization was mainly a side note in the field of photopolymerization until the mid 1970s. They were mainly employed by Americure Technology and commercially used for coating on metal cans.²³ The photoinitiators used to absorb the light and generate the cationic active centers (such as aryldiazonium salts) were very costly, had poor stability (meaning they would spontaneously gel in the absence of light due to internal thermal instability) and would produce nitrogen gas during their initiation causing pinholes and deteriorating properties of the polymer.²³ These initiator deficiencies prevented cationic photopolymerization use in any practical application despite having significant advantages over free radical photopolymerization.

The potential of the cationic photopolymerizations spurred research into overcoming the cationic photoinitiator problems. In parallel investigations, two companies, 3M and General Electric, developed and patented new classes of cationic photoinitiators; diaryliodonium salt photoinitiators and triarylsulfonium salt photoinitiators. These initiators are quite thermally stable for a wide range of temperatures, highly photosensitive (absorb light very efficiently with optical yield above ~0.7), inexpensive to create and purify, and produce no gas upon reaction. By solving the previous cationic photoinitiator problems, cationic photopolymerization could become a viable option commercially. This new market was spilt by the patent office by awarding G.H. Smith from 3M the patent for the diaryliodonium salt photoinitiator²⁴ and J.V. Crivello from General Electric Corporation the patent for the triarylsulfonium salt

photoinitiators.²⁵ The two companies settled on an agreement to have a mutual cross-license of the technologies and the production of stable, efficient cationic photoinitiators began.²³

The commercial availability of the new cationic photoinitiators meant cationic photopolymerization could realistically be implemented in industrial application. This possibility stimulated research in this field. Research into the kinetics, mechanisms, and physical properties of cationic photopolymerization began with the ultimate goal of having them replace free radical photopolymerization. Cationic monomers were studied to see if reaction rates and properties could rival that of free radical photopolymerization. The initial research was mainly on the more common cationic monomers, epoxides and vinyl ethers. It was found that vinyl ethers have very fast photopolymerization rates rivaling free radical rates but often lead to uncontrollable runaway reactions.⁵ Due to this unmanageable aspect, vinyl ethers are typically shunned by industry. Conversely, epoxide cationic photopolymerizations are very controllable and give fantastic physical properties, but the photopolymerization rate is very slow in comparison to vinyl ethers and free radicals monomers. It was found increasing the ring strain (such as using a cycloaliphatic epoxide) promotes the ring opening polymerization reducing the overall polymerization time. This caused 3,4-epoxycyclohexylmethyl-3',4'-epoxycyclohexane carboxylate to become an industrial standard for its high reactivity and good physical properties.⁵ Despite this increase in reactivity cationic photopolymerization were still about 10 times slower than free radical photopolymerizations.³

Further investigation into new cationic monomers has found promise in siloxanes (a molecule with a dimethyl siloxane between the two cyclo-epoxide groups) and oxetanes (a molecule with a four member oxygen ring). Siloxanes have shown to have cure speeds rivaling free radical polymerization without the loss of the cationic superior physical properties.^{3,26}

Oxetanes have similar ring strain to epoxides. However their basicity is much greater, yielding improved polymerization times and conversions over epoxides.²⁷ Beyond these new monomers, several hybrid free radical/cationic photopolymerization have also been investigated as a means to create a variety of novel polymers and develop a system which overcomes the limitations of the individual reactions and combines their advantages.⁷

The focus of cationic photopolymerization research has shifted away from developing higher/ faster reaction rates to focusing on cationics' more unique aspect, their long lived active centers. Decker and Moussa studied the active center lifetimes of both the long lived cationic active centers and the extremely short lived free radical active centers.^{3,7,8,9,18} In addition to characterizing these lifetimes, the scientists studied several cationic systems for their ability to dark cure and the property development due to the dark cure.^{3,22,28,29} In a study of a diepoxide system, they found dark cure can account for 80% of the polymer formed.²²

Spani *et al.* also studied the cationic active centers' ability to dark cure. They used this dark cure ability to develop a new method of obtaining cationic rate termination and propagation constants as well as active center lifetimes for cationic polymerizations.^{30,31} The effects of photoinitiators, monomer structure and crosslinking on dark cure were also examined.

Information gleaned from all this research allowed cationic photopolymerization to be applied in a number of fields. Cationic cure has been used in metal coatings since it offer excellent adhesion, chemical resistance and high gloss appearance. In 1996, the Coor Brewing Company was coating 4 billion cans per year using cationic photopolymerizations.²³ Another large application of cationic photopolymerization is stereolithography. Stereolithography creates polymer three dimensional objects by successively curing one thin layer on top of the other.³² Cationic photopolymerizations are used in this field due to their low shrinkage, low toxicity and

excellent mechanical properties. Cationic photopolymerization dark cure properties have established themselves in a number of laminate and pressure sensitive adhesives applications where the adhesive continues to cure long after the light has been removed.³ Cationic photopolymerizations are also growing in the market of ink jets for their physical properties and their ability to dark cure.^{33,34}

Though cationic photopolymerization is being applied in many fields, the full potential of the unique cationic active centers have not yet been realized. Exploring the relatively un-researched area of cationic active centers lifetimes and mobility and understanding the fundamentals behind their migration will lead to the realization of many exciting possibilities in the fields where previous photopolymerization problems have barred them.

CHAPTER 2. OBJECTIVES

Photopolymerization, with its many advantages over traditional thermopolymerization is well-established as the preferred option for a variety of film and coating applications. Photopolymerization is only favored in these applications because they all require only thin, optically clear coatings on geometrically simple substrates. Applications beyond these parameters (such as thick or pigmented coatings on complex shapes) are presently inaccessible to photopolymerization due problems with light attenuation, additive interference, and shadow regions.

The overall objective for this research was to demonstrate that the problems of light attenuation, additive interference, and shadow regions could be solved and new applications obtained by utilizing cationic photopolymerizations' unique active centers. To reach this overall objective, more specific intermediary objectives had to be realized. These specific objectives include:

- (i) proving that the long-lived cationic active centers can migrate through a thick monomer system, curing in regions that never receive illumination;
- (ii) demonstrating how this migration can lead to the efficient photopolymerization of pigmented systems;
- (iii) establishing methods for using the long lifetimes of cationic active centers to photopolymerize coatings on complex shapes, and create sequential stage curable polymers;
- (iv) developing a technique for external temporal control of the photopolymerization after the illumination has ceased.

CHAPTER 3. ABILITY OF CATIONIC PHOTOPOLYMERIZATIONS TO CURE THICK SYSTEMS THROUGH ACTIVE CENTER MIGRATION

3.1. Introduction

Photopolymerization, with its many advantages, has been relatively unemployed in thick polymer applications (greater than 1 cm) due to light attenuation. Light attenuation is where the intensity of the light falls off through space as it is absorbed by the photoinitiator. This means the photons being absorbed by the photoinitiators closer to the illumination source reduce the number of photons that can reach the photoinitiators located in the deeper regions of the sample. This attenuation decreases both the maximum rate of photoinitiation and stagnates the production of active centers throughout the sample.

In this chapter, the long-lived cationic active centers that are responsible for dark cure will be investigated for their ability to “shadow cure” in unilluminated regions of the thick sample. “Shadow cure” occurs when the active centers migrate out of the illuminated region (through a combination of diffusion and reaction) into the deep shadow regions of the sample, thereby polymerizing the unexposed monomer. The ability to shadow cure could overcome many of photopolymerization’s current shortcomings including the problem of light attenuation in larger sample depths. A series of systematic studies are presented to find the spatial profile of the cationic photopolymerization active centers production, investigate the cationic active center migration, and characterize the shadow cure of thick polymer systems.

3.2. Modeling the Spatial Profile of Active Centers Production

Cationic photopolymerizations are unique for creating the essentially non-terminating active centers. The long lifetimes of these active centers can be used in numerous ways such as dark and shadow cure. To understand how dark cure and shadow cure function, first the

knowledge of where the active centers are being produced within a sample must be understood. This is a complex process especially for thick systems, that is influenced by many factors including lamp emission, photoinitiator absorbance, photolysis products absorbance (photobleaching effect), light intensity, etc. For accurate description of the spatial photoinitiation profiles produced during the illumination step, the finite difference analytical method reported by Kenning *et al* was modified and used.^{16,35} This analysis is based upon the set of fundamental differential equations that govern the evolution of the light intensity gradient and initiator concentration gradient for multi-wavelength illumination. This analysis originally was created to model the active center production in free radical photopolymerization. It was used to study the influence of formulation factors such as initiator concentration, absorptivity, quantum yield, absorbance by the monomer, absorbance by the initiator fragments, diffusion of the initiators and fragments and photobleaching and non-photobleaching additives. The influence of the light source was also studied by performing the analysis for several initiator/light source combinations, monochromatic or polychromatic light, illumination from one or two sides, intermittent illumination and with a reflective substrate. This versatile model was easily modified and used to model not just the cationic active center production, but, since cationic active centers have essentially no termination, the overall concentration of the active centers as well.

3.2.1. Governing Differential Equations

The basis of this active center generation model is a set of differential equations, given below, that describe the evolution of the light intensity gradient and initiator concentration gradient for multi-wavelength illumination.

$$\frac{\partial C_i(z, t)}{\partial t} = -\frac{C_i(z, t)}{N_A h} \sum_j \left(\frac{\varepsilon_{ij} \phi_j I_j(z, t)}{\nu_j} \right) + D_i \frac{\partial^2 C_i(z, t)}{\partial z^2} \quad (3.1)$$

$$\frac{\partial C_p(z, t)}{\partial t} = \frac{C_i(z, t)}{N_A h} \sum_j \left(\frac{\varepsilon_{ij} \phi_j I_j(z, t)}{\nu_j} \right) + D_p \frac{\partial^2 C_p(z, t)}{\partial z^2} \quad (3.2)$$

$$\frac{\partial I_j(z, t)}{\partial z} = -[\varepsilon_{ij} C_i(z, t) + A_{mj} + A_{aj} + \varepsilon_{pj} C_p(z, t)] I_j(z, t) \quad (3.3)$$

Here, the subscript j is an index indicating the wavelength of light under consideration; $C_i(z, t)$ is the initiator molar concentration at depth z and time t ; $C_p(z, t)$ is the photolysis product molar concentration at depth z and time t ; $I_j(z, t)$ is the incident light intensity of a specific wavelength at z and t with units of energy/(area*time); ε_i is the initiator Napierian molar absorptivity of a specific wavelength with units of volume/(length*mole); ε_p is the photolysis product Napierian molar absorptivity of a specific wavelength with units of volume/(length*mole); ϕ is the quantum yield of the initiator, defined as the fraction of absorbed photons that lead to fragmentation of the initiator; N_A is Avogadro's number; h is Planck's constant; ν is the frequency of light in units of inverse seconds; D_i is the diffusion coefficient of the initiator in units of length²/time; D_p is the diffusion coefficient of the photolysis products; A_m is the absorption coefficient of the monomer and the polymer repeat unit with units of inverse length; and A_a is the absorption coefficient of any additives into the system like pigments, UV stabilizers, etc. Note that the Napierian molar absorptivity was adopted because it is most natural for the differential version of the absorption equation.

For an accurate description of initiation with polychromatic illumination, the light intensity gradient at each incident wavelength must be individually described. As shown in equation 3.3, the intensity of an individual wavelength is attenuated by absorption of the initiator, monomer, additives, and the photolysis product. Since the local initiator concentration

depends upon all of the incident wavelengths, and the local light intensity of each wavelength depends upon the initiator concentration, the time-evolution of all of the light intensities are coupled to one another, and therefore the complete set of differential equations must be solved simultaneously. Therefore, the wavelength dependence of the intensity considerably increases the complexity of the model; for description of n wavelengths of incident light, $n+2$ equations must be solved simultaneously.

The following initial and boundary conditions apply to this system:

$$C_i(z,0) = C_o \quad (3.4);$$

$$C_p(z,0) = 0 \quad (3.5);$$

$$\frac{\partial C_{i,p}}{\partial z} = 0 \text{ at } z = 0 \text{ and } z = z_{\max} \quad (3.6);$$

$$I(0, t) = I_o \quad (3.7).$$

Equation 3.4 states that the initial initiator concentration is uniform throughout the depth of the sample. Similarly, Equation 3.5 indicates that the initial photolysis product concentration is zero. Equation 3.6 is the no-flux boundary condition indicating that there is no diffusion through the ends of the sample at each time, and equation 3.7 states that at any time, the intensity on the sample's surface where the light enters is equal to the initial intensity of the light source.

Simultaneous solution of equations 3.1-3.3 under the boundary conditions of equations 3.4-3.7 yields profiles for the instantaneous light intensity gradients at each incident wavelength and initiator concentration gradient at any time. At a given location in the sample, the local rate of active center production, described by equation 3.8, can be found using these gradients.

$$R(z,t) = C_i(z,t) \sum_j [I_j(z,t)] \phi_j \varepsilon_{ij} \quad (3.8).$$

Here $R(z,t)$ is the local rate of active center production at depth z and time t (mole/(volume*time)), the subscript j is an index indicating the wavelength of light under consideration, and the other symbols have been defined above. This equation illustrates that the

local rate of active center generation is proportional to the local initiator concentration, and depends upon the light intensity at each initiating wavelength.

Since the cationic active centers are essentially non-terminating, and active center diffusion is negligible for timescales of several minutes, the cationic active center concentration profile at a given time, t , can be found by integrating equation 3.8 from zero to t . This means wherever cationic active centers are created they will continue to be located, unlike free radicals which would quickly disappear from termination reactions.

3.2.2. Modeling a Standard Cationic Photoinitiator/Monomer System

This analysis is a very good tool for determining initial spatial profiles of active centers and therefore thickness of a sample after illumination. The cationic monomer, 3,4-epoxycyclohexylmethanyl 3,4-epoxycyclohexanecarboxylate (CDE, Figure 3.1, Dow Chemical Co.) and photoinitiator, (tolcumyl) iodonium tetrakis (pentafluorophenyl) borate (IPB, Figure 3.2, Secant Chemicals Inc.) initial active center profiles was modeled using the equations above.

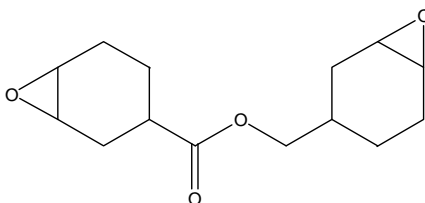


Figure 3.1. Molecular structure of 3,4-epoxycyclohexylmethanyl 3,4-epoxycyclohexanecarboxylate.

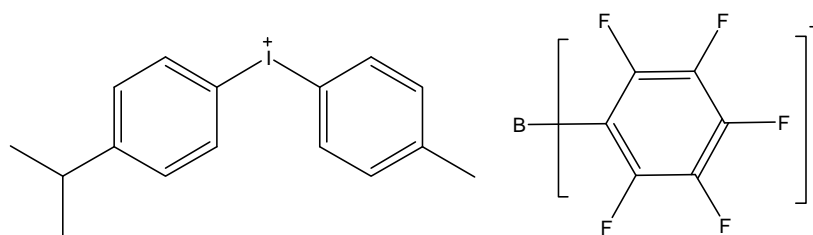


Figure 3.2. Molecular structure of (tolcumyl) iodonium tetrakis (pentafluorophenyl) borate.

UV-Visible absorption spectra were obtained for the monomer and photoinitiators using an Agilent Model 8453 UV-Visible Spectrophotometer. The spectra were obtained for a dilute solution ($\sim 10^{-2}\text{M}$, $\sim 10^{-5}\text{M}$, respectively) of each compound in methanol at room temperature. The resulting spectra were analyzed to determine the molar absorptivity of each compound at the wavelengths active for photoinitiation. As described below, the molar absorptivities were used to determine the light penetration and active center generation profiles during the illumination. The molar absorptivity of this photoinitiator was determined at one nanometer increments using an Agilent UV-Visible spectrometer. This spectrum is shown in Figure 3.3.

The lamp used to illuminate the sample was a medium pressure 200 Watt Hg-Xe arc lamp (Oriol). The relative emission intensities of the lamp was determined at one nanometer increments using an Ocean Optics spectrometer, and the resulting emission spectra is shown in Figure 3. The wavelengths that the lamp emits and the photoinitiator absorbs are the primary wavelengths that produce active centers. These wavelengths are $\sim 295\text{-}307\text{nm}$ for this example. Below 295nm the lamp is not emitting as strongly and the monomer will absorb any photons that the lamp does emit while above 307nm the photoinitiator does not absorb.

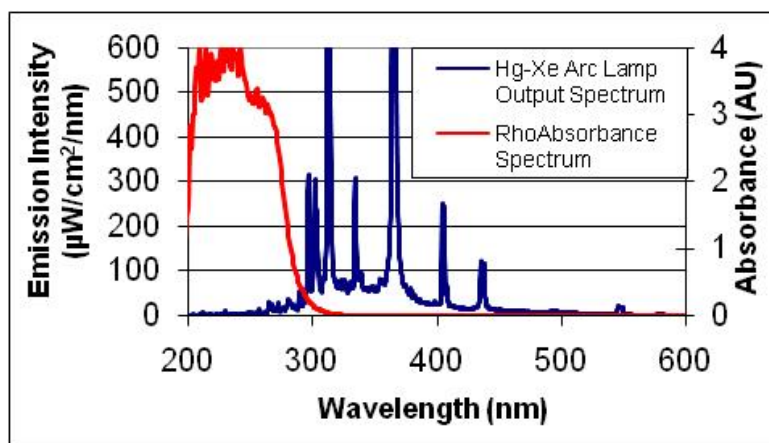


Figure 3.3. Spectra for the Hg-Xe arc lamp emission and the photoinitiator IPB absorbance.

Using the information obtained from photoinitiator absorptivity and the HgXe arc lamp emission spectrum, the simultaneous solution of equations 3.1-3.3 yields profiles for the instantaneous light intensity gradients at each incident wavelength and initiator concentration gradient at any time. Figure 3.4 shows profiles of the total light intensity (summed over all incident wavelengths) and the photoinitiator concentration for illumination times ranging from 0 to 5 minutes. These modeling results illustrate that the initial photoinitiator concentration is uniform (21 g/L or 0.023 mol/L) and the initial light intensity gradient falls off in accordance with Beer's Law summed over the incident wavelengths, and penetrates approximately 0.1 mm into the sample. As time progresses, the photoinitiator at the illuminated surface becomes completely consumed (the concentration goes to zero) while the concentration at larger depths remains unchanged. Therefore, the photoinitiator concentration profile assumes a sigmoidal shape, with the depth of the inflection point increasing with time. The shape of the light intensity profile arises from a combination of the absorption by the monomer (which leads to the gradual reduction in light intensity beginning at the illumination surface), and the absorption by the photoinitiator (which causes the severe drop on light intensity to zero).

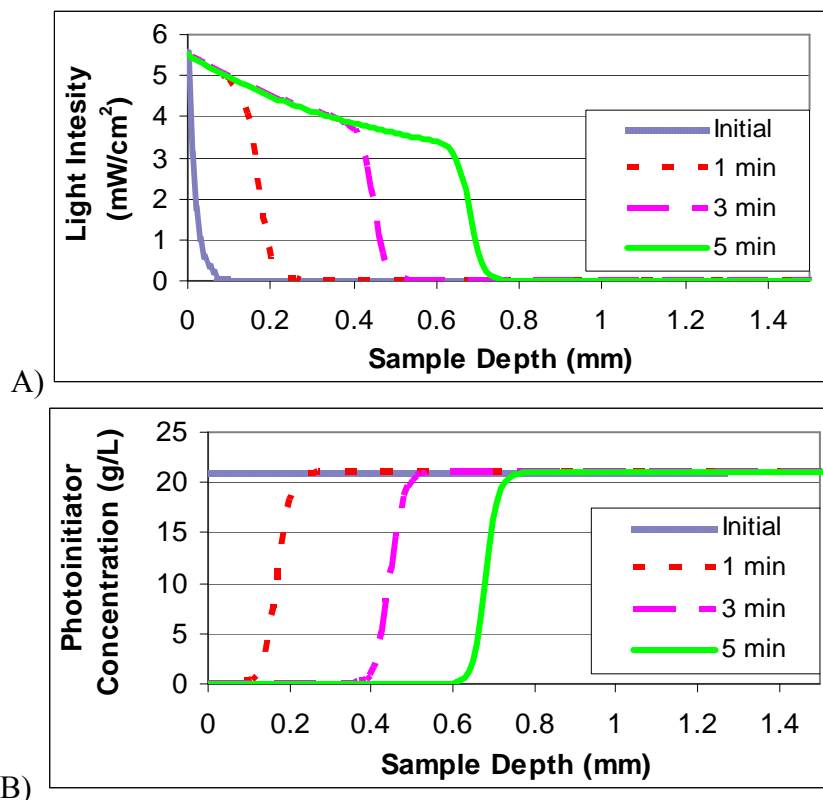


Figure 3.4. Evolution of profiles during illumination for: A) the total light intensity summed over the initiating wavelengths (295-307 nm) and B) the photoinitiator concentration. Monomer: CDE, Initiator: 0.5 mol% IPB, Exposure time: 5 min, Exposure temp.: 25°C, Intensity: 50mW/cm²

Profiles, found from Equation 8, for the rate of active center production for illumination times ranging from 1 to 5 minutes are shown in Figure 3.5. At a given time (*e.g.* five minutes of illumination) the active center generation rate is zero at the illuminated surface because the local photoinitiator concentration is zero (it was previously consumed), and is zero for large depths for which the total light intensity is zero. Therefore, the profile for the instantaneous rate of active center generation has a local maximum or peak value, and moves like a wave from the illumination surface toward the top of the sample. Note that the maximum rate at the wave peak decreases slowly with time due to absorption of light by the monomer.

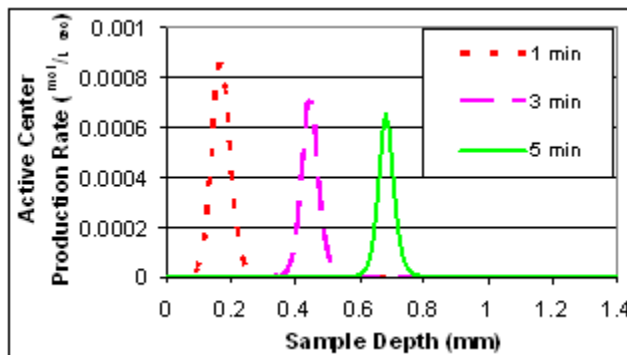


Figure 3.5. Evolution of active center rate production profiles during illumination. Monomer: CDE, Initiator: 0.5 mol% IPB, Exposure temp.: 25°C, Intensity: 50mW/cm²

Figure 3.6 shows cationic active center concentration profiles for illumination times up to 5 minutes, and illustrates that the cationic active centers are first generated at the illuminated surface of the sample with a sharp drop in active center concentration to a value of zero at the leading edge of the illumination front. Note that the maximum active center concentration is equal to the initial photoinitiator concentration (0.023 moles/liter) since each photoinitiator molecule leads to the formation of a single cationic active center. Based upon this analysis, after five minutes of illumination, the region of the sample beyond 0.7 mm of depth has an active center concentration of zero and is therefore in the shadow region of the sample. This reliable method for obtaining the initial spatial profiles of the active centers established the foundation for investigations into the active center migration and photopolymerization of thick polymer systems.

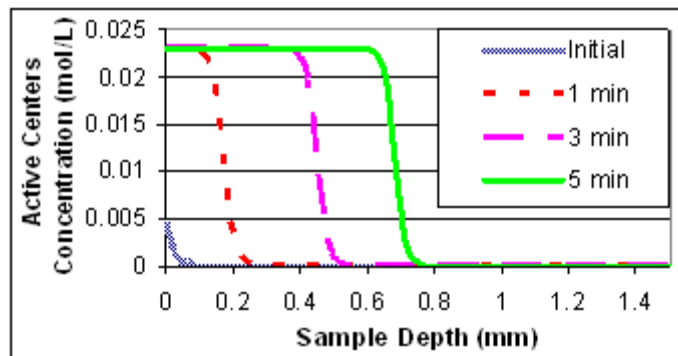


Figure 3.6. Evolution of the active center concentration profiles during illumination. Monomer: CDE, Initiator: 0.5 mol% IPB, Exposure time: 5 min, Exposure temp.: 25°C, Intensity: 50mW/cm²

3.3. Active Center Mobility through Thick Polymer Systems

Cationic photopolymerization has essentially no termination leading to extremely long active centers lifetimes. The long lifetimes of these active centers have the potential to be mobile and migrate out of the illuminated region into the deep shadow regions of the sample thereby polymerizing the unexposed monomer in a process termed as “shadow cure”. To understand and control this ability, the fundamental driving force behind the active center migration must be found along with the effect of several different variables. With this knowledge, the migration of the shadow cure could be predicted and used effectively to overcome many of photopolymerization’s current shortcomings including the problem of curing of thick polymer systems.

3.3.1. Active Center Migration Experiments

3.3.1.1. Materials

The cationically polymerizable monomer 3,4-epoxycyclohexylmethanyl 3,4-epoxycyclohexanecarboxylate, (CDE, Figure 3.1, Aldrich) was used in these experiments. This monomer was selected for its high reactivity and low shrinkage. Two photoinitiators used in this

study were: (tolycumyl) iodonium tetrakis (pentafluorophenyl) borate (IPB, Figure 3.2, Secant Chemicals) and diaryliodonium hexafluoroantimonate (IHA, Figure 3.7, Sartomer). These two photoinitiators were selected for these studies because they are two of the most effective commercially available cationic photoinitiators (photolysis yields of 0.7-0.9)²³, and because their counter-ions are significantly different in size.

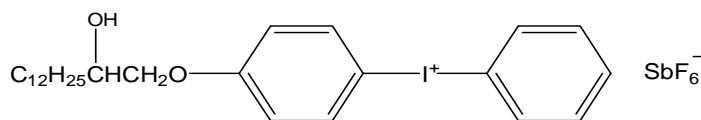


Figure 3.7. Molecular structure of diaryliodonium hexafluoroantimonate.

3.3.1.2. Photopolymerization

Photopolymerizations were initiated using a 200 W Oriel Hg(Xe) arc lamp. The output of the lamp was passed through a water filter to eliminate infrared light, and the resulting irradiance of the lamp measured to be 50.0 mW/cm^2 . The photopolymerizations were carried out under atmospheric conditions and at room temperature.

3.3.1.3. Characterization of Shadow Cure

The extent of shadow cure as a function of time was characterized for a variety of temperatures, exposure times, photoinitiators and photoinitiators concentrations. These experiments were performed using disposable 4.5 ml polystyrene cuvettes, which were chosen because they are transparent to the wavelengths of interest and will readily dissolve in a number of solvents, therefore allowing the extent of polymerization to be easily determined. Each monomer-filled cuvette (filled to a level of ~3 cm) was illuminated from below with the light from the 200 W Hg/Xe lamp for a prescribed duration (the exposure time, typically five

minutes). Since the density of the polymer is higher than that of monomer, illumination from below avoids polymerization-induced convection or mixing. After exposure, the system was maintained at the prescribed temperature (monitored by micro-dot irreversible temperature Indicators from Omega Co.) for the predetermined shadow cure time. In every cuvette, the polymerization was observed to begin at the bottom of the sample (due to the illumination from below with a penetration depth no more than ~millimeter) and moved as a polymerization front toward the top of the sample (into the unilluminated shadow region).

At the prescribed shadow cure time, the sample was placed in tetrahydrofuran (THF) to dissolve the uncured region of the sample. In this highly-crosslinked system, monomer becomes incorporated into the polymer matrix as it reacts with active centers, so essentially no soluble polymer fraction exists. The insoluble crosslinked polymer matrix was washed with acetone to remove any remaining THF and excess monomer. The polymer sample was dried thoroughly and its weight was recorded. The polymerized thickness was determined by dividing the weight of the polymer sample by the product of the polymer density and the area of illuminated surface (the cross-sectional area of the cuvette, 1.0 cm²). At each temperature and shadow cure time, an unilluminated control sample was prepared to verify that thermally-induced polymerization did not occur.

3.3.2. Active Center Migration Results and Discussion

3.3.2.1. Time Dependence of Shadow Cure

To characterize the extent of shadow cure as a function of time, a one dimensional study was carried out using the monomer cycloaliphatic diepoxide under the experimental conditions described above. Representative experimental results are shown in Figure 3.8. In this figure, the initial polymer height after five minutes of illumination (calculated to be 0.7 mm using the

method described in the previous section) is illustrated by the solid portion of each bar. The striped portion of each bar indicates the observed additional cure (the shadow cure distance) as a function of the shadow cure time (time zero corresponds to the instant at which the illumination is ceased). Multiple independent samples were measured for each time, and the resulting standard deviations are indicated as the error bars on the graph. The figure illustrates clearly that as the shadow cure time is increased, the height of polymerized sample increases (from ~3 mm in 0.5 hours to ~7 mm in 8 hours). In each case, the polymerization progresses as a reaction front which extends upward from the illuminated surface at the bottom of the sample. A control sample which contains all reaction components but is never illuminated, remained as unpolymerized liquid monomer for the entire duration of the experiment.

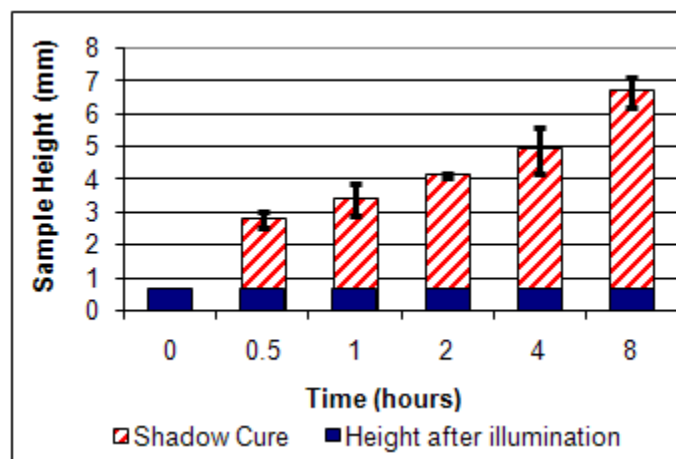


Figure 3.8. Proof of shadow cure; sample heights over time with no additional illumination. Monomer: CDE, Initiator: IPB 0.5 mol%, Exposure time: 5 minutes, Exposure temp.: 25°C, Intensity: 50mW/cm², Shadow Cure Temperature: 50°C.

The data in Figure 3.8 illustrate that shadow cure does indeed occur in this cationic photopolymerization of a thick cycloaliphatic diepoxide monomer, and that it progresses from the illuminated surface into the shadow regions due to the mobility of the active centers. During

the illumination time, cationic active centers are produced in the illuminated region, and propagate to polymerize the surrounding monomer. Since chemical termination is practically nonexistent in cationic photopolymerization, the long lived active centers have time to migrate into the shadow region and cause the polymerization front to move. Therefore cationic migration leads to further polymerization in the unilluminated region in the frontal nature observed in the experiment.

To characterize the active center mobility and migration that leads to shadow cure, it is useful to examine data for the time-dependency of the shadow cure distance (which corresponds to the diagonal-striped area in Figure 3.8). A plot of the shadow cure distance as a function of time using a linear time axis (Figure 3.9A) reveals that the slope of the curve decreases with increasing time in a manner consistent with a diffusional process. In general, the diffusion distance increases with the square-root of time, and Figure 3.9B illustrates that the data exhibit a good fit to this relationship. Fitting the experimental data to the diffusion equation yields an effective shadow cure diffusion coefficient of $9.2 \times 10^{-6} \text{ cm}^2/\text{sec}$, which is fast for solute diffusing in a polymer matrix.³⁶ While the active center mobility is certainly more complex than a solute diffusing through a polymer matrix, consideration of the underlying physical picture reveals that it is reasonable for the active center mobility to generally follow a diffusional dependency. Even though the active centers are covalently linked to an immobile highly crosslinked matrix, they retain mobility through “reactive diffusion” in which the active centers migrate by propagating with unreacted monomers (or with pendent epoxide groups). Reactive diffusion has been shown to provide an important mode for active center mobility in free radical polymerizations of multifunctional acrylates^{37,38} and cationic polymerizations of divinyl ethers.^{39,40} Since the shadow cure progresses in a frontal manner, a second diffusional process that may effect that

shadow cure distance at a given time is the diffusion of monomer into the polymer matrix at the leading edge of the front. Since the active center must be able to access unreacted monomer for reactive diffusion to occur, it is difficult to isolate the contribution of monomer diffusion. Therefore, the effective shadow cure diffusion coefficient likely depends upon contributions from both monomer diffusion and reactive diffusion (which depends upon the rate of propagation).

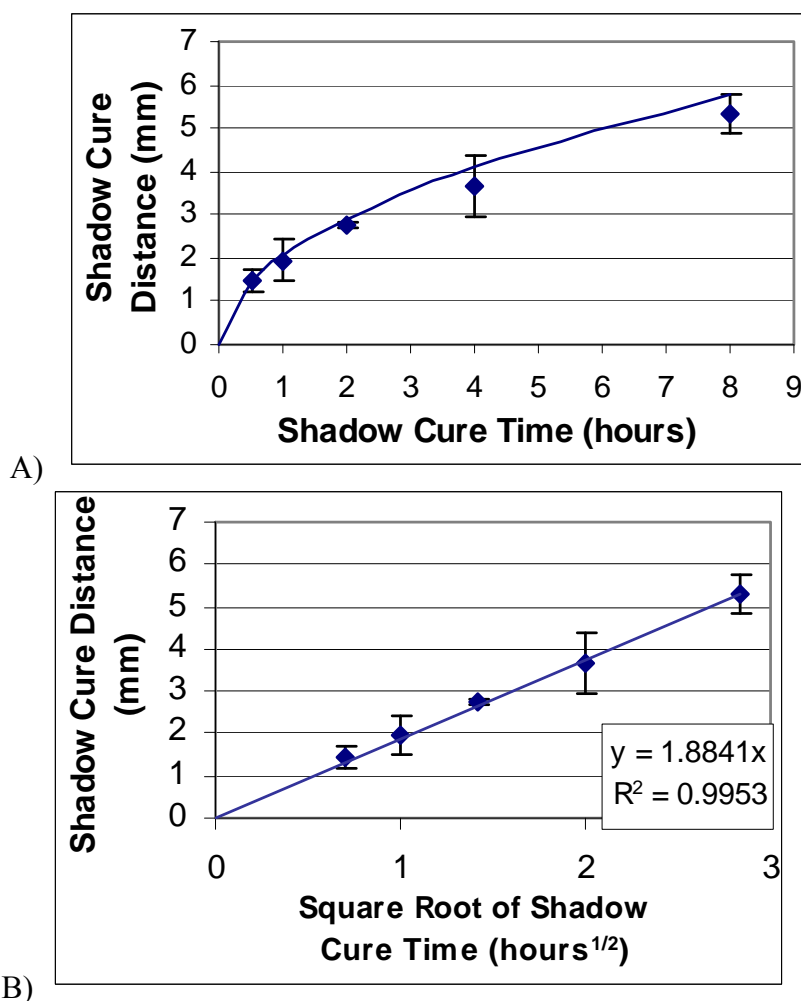


Figure 3.9. Shadow cure dependence on time: A) linear time axis and B) square root time axis. Monomer: CDE, Initiator: 0.5 mol% IPB, Intensity: 50 mW/cm², Exposure time: 5 min, Exposure temperature: 25°C, Shadow cure temperature: 50°C

3.3.2.2. Effect of Temperature

A series of experiments was performed to characterize the effect of temperature on the active center mobility. The only condition changed was the temperature the sample was stored at after illumination. This allows for the temperature effect on only the active center migration to be studied, not its effect on the initial active center production. Figure 3.10 contains profiles of the shadow cure distance as a function of the square root of time for temperatures ranging from 30 to 60°C at ten degree intervals. For each temperature, the best-fit line is shown, and the corresponding effective shadow cure diffusion coefficients are: 6.9×10^{-7} , 3.0×10^{-6} , 9.2×10^{-6} , and 2.4×10^{-5} cm²/sec for temperatures of 30, 40, 50, and 60°C, respectively. The temperature dependence of the effective shadow cure diffusion coefficient was well described by the Arrhenius relationship with an activation energy of 89 kJ/mol as shown in Figure 3.11. This value is close to the activation energy of propagation for cationic ring-opening polymerizations of oxiranes in highly crosslinked systems.⁴ Therefore, the temperature dependence of the effective shadow cure diffusion coefficient is consistent with the hypothesis that the active center mobility is facilitated by reaction diffusion.

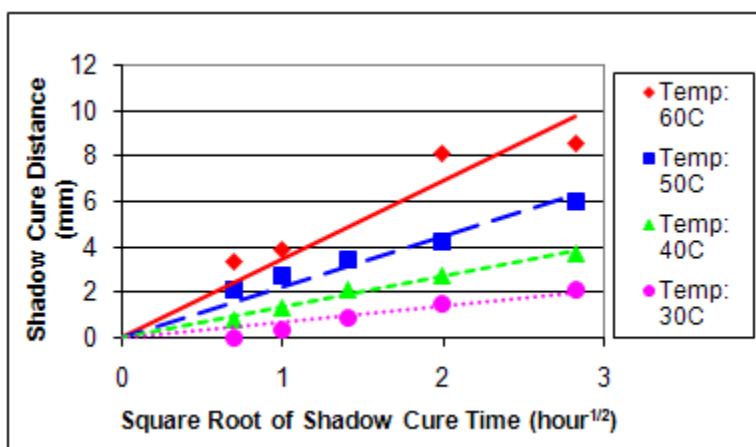


Figure 3.10. Effect of temperature on shadow cure. Monomer: CDE, Initiator: 0.5 mol% IPB, Intensity: 50 mW/cm², Exposure time: 5 min, Exposure Temp.: 25°C

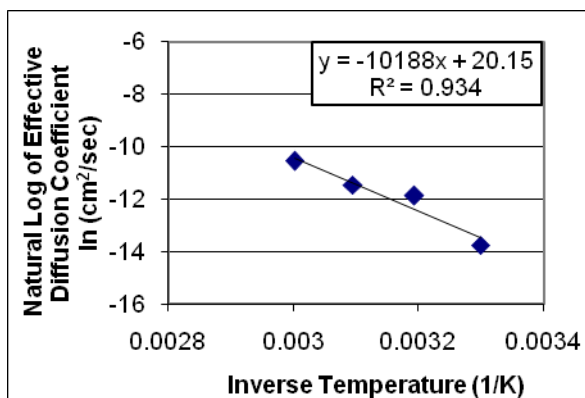


Figure 3.11. Arrhenius relationship between temperature and effective diffusion coefficient. Monomer: CDE, Initiator: 0.5 mol% IPB, Intensity: 50 mW/cm², Exposure time: 5 min, Exposure Temp.: 25°C

3.3.2.3. Effect of the Photoinitiator Counter-ion

The photoinitiator counter-ion provides a convenient method for investigating the role the polymerization rate (which controls the rate of reaction diffusion) on the extent of shadow cure. It is well established that the counter-ion plays an important role in determining the propagation kinetic constant, with higher values arising from larger counter-ions. Therefore, changing the photoinitiator counter-ion provides a means for changing the kinetic constant for propagation while leaving all other variables unchanged.

Spatial profiles of the cationic active center produced during illumination were generated for two iodonium salts to verify that changing counter-ion will not affect the initial spatial profile. The two photoinitiators used in this study were IPB and IHA. The (pentafluorophenyl) borate counter-ions of the IPB are approximately 14% larger by volume than the hexafluoroantimonate counter-ion. Despite this difference in counter-ion size, the absorbance of the two photoinitiators and the resulting initial active centers production spatial profiles remain essentially the same as seen in Figure 3.12. These results demonstrate that the two iodonium salts create essentially the same spatial profile of active centers available to migrate.

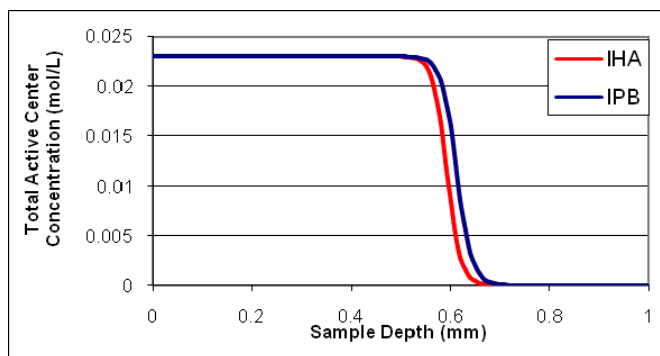


Figure 3.12. Active center concentration profiles of photoinitiators with different counter-ions. Monomer: CDE, Initiator: 0.5 mol% IPB or IHA, Exposure time: 5 min, Intensity: 50mW/cm²

A series of experiments were performed to investigate the shadow cure as a function of time for dicycloaliphatic epoxides initiated using these two different photoinitiators. The results illustrated in Figure 3.13 show that the extent of shadow cure is much higher in the system initiated by IPB than the system initiated by IHA. The effective shadow cure diffusion coefficients for IHA and IPB at 50°C were found to be 4.0×10^{-7} and 9.2×10^{-6} cm²/sec, respectively. The fact that the system with the higher propagation rate constant (all other variables held constant) also exhibits a higher shadow cure progression rate is consistent with the conclusion that the active center mobility arises largely from reactive diffusion.

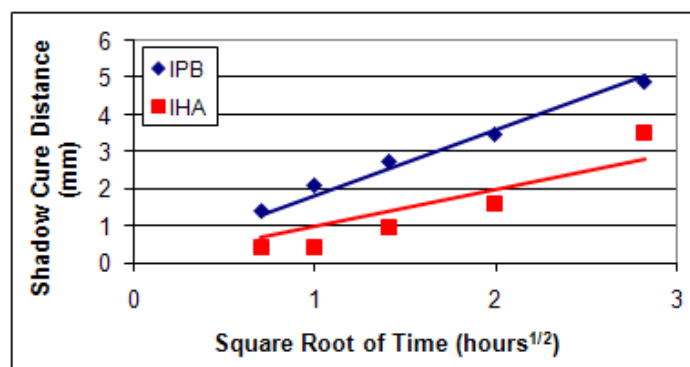


Figure 3.13. Effect of photoinitiator counter-ion on shadow cure. Monomer: CDE, Initiator: 0.5 mol%, Intensity: 50 mW/cm², Exposure Time: 5 min, Exposure Temp.: 25°C, Storage Temp.: 50°C.

3.3.2.4. Effect of Photoinitiator Concentration

The photoinitiator concentration is another variable that can affect the cationic active center's ability to polymerize thick systems. The IPB photo-initiator concentration was varied from 0.0125 to 0.75 mol % for these experiments. The effect of IPB concentration has on the initial spatial active center profile is shown in Figure 3.14. In this figure, the initial concentration of active centers changes for each photoinitiator concentration. However, the total number of active centers created (area beneath the curves) remains approximately constant because as the initiator concentration increases, the depth the light is able to penetrate reduces which keeps the moles of the initiator exposed stable. This means the initial number of active centers is $\sim 1.3 \times 10^{-3}$ moles and remains constant. So the analysis of the initial spatial profile reveals that while spatial profile are changed, the total amount of active center generated is the same.

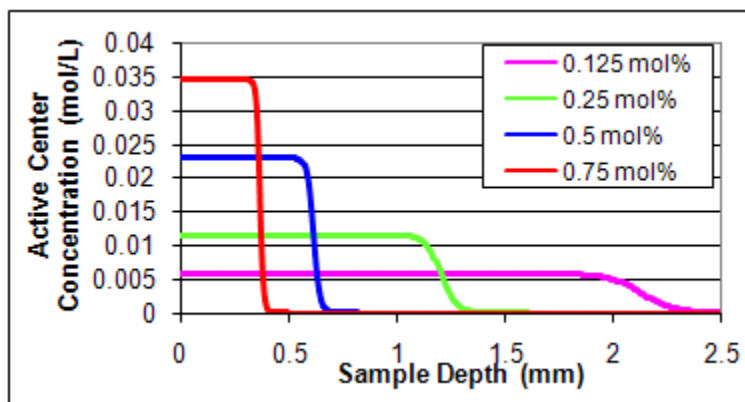


Figure 3.14. Active center concentration profiles of different photoinitiators concentrations. Monomer: CDE, Initiator: IPB, Exposure time: 5 min, Exposure temp.: 25°C, Intensity: 50mW/cm²

The influence of the initiator concentration on the cationic active center migration was investigated as well as the active center production. The initiator concentrations studied were

varied from 0.0125 to 0.75 mol % and their effects on the shadow cure were placed in Figure 3.15. The data reveals that an increase in initiator concentration increases the system's ability to shadow cure despite creating the same number of active centers. This increase is due to the gradient of active centers (the concentration of active centers on the edge of the sample). The gradient or the concentration difference between the illuminated area and the shadow region is responsible for diffusion. Therefore, any increases to gradient will increase the diffusional driving force, compelling the active center to migrate faster.

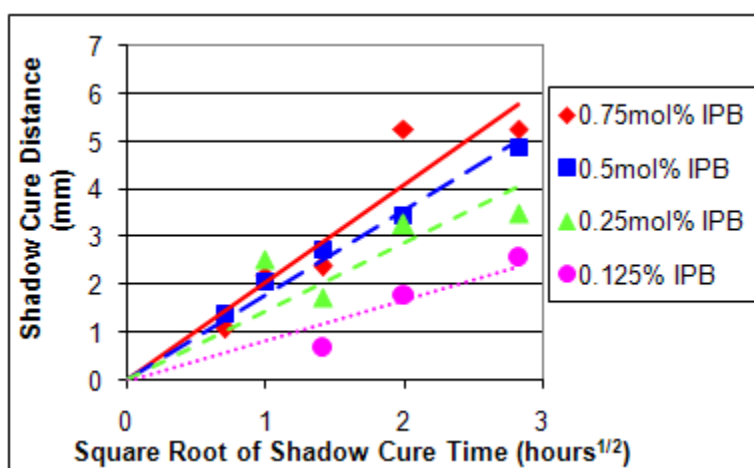


Figure 3.15. Effect of photoinitiator concentration on shadow cure. Monomer: CDE, Initiator: IPB, Intensity: 50 mW/cm², Exposure time: 5 min, Exposure Temp.: 25°C, Storage Temp.: 50°C

3.3.2.5. Effect of Exposure Time

Since increasing the concentration of the photoinitiator does not increase the number of active centers generated, another method must be employed to find the effect of total active center concentration on migration and shadow cure. Increases in exposure time, increases the total number of active centers produced in the sample and the depth at which active centers are created, yet the active center spatial profile remains the same (see Figure 3.6). The effect of the illumination time (and subsequent active center concentration) on shadow cure was investigated

and the results are shown in Figure 3.16. Since the shadow cure distance is measured from the initial depth, the increase in shadow cure does not arise directly from light penetration, but rather from the mobility of the active centers that were produced. Figure 3.16 shows that as the exposure time is increased from 2 to 6 minutes, the extent of shadow cure is increased. At longer illumination times, the total number of active centers is increased which leads to an enhanced driving force for diffusion. A measure of this driving force is indicated by the diffusion coefficient or slope of the line. Enhancing the driving force behind the cationic active centers mobility enhances the mobility and corresponding extent of shadow cure.

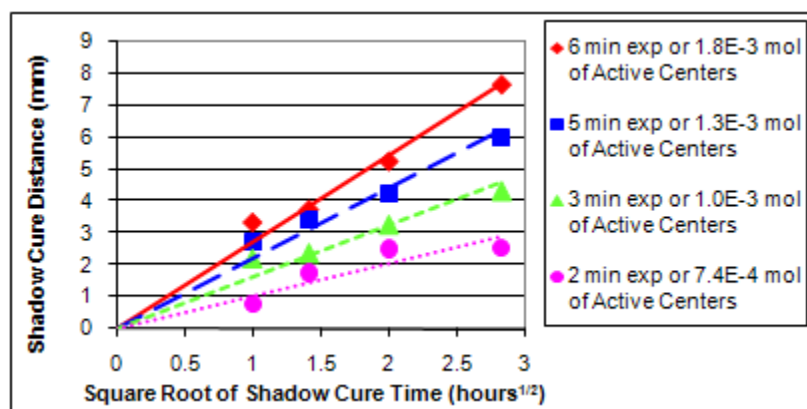


Figure 3.16. Effect of the exposure time on shadow cure. Monomer: CDE, Initiator: 0.5 mol% IPB, Exposure temp.: 25°C, Intensity: 50mW/cm², Shadow Cure Temperature: 50°C.

3.4. Modeling Active Center Mobility through Thick Polymer Systems

An accurate fundamental theoretical model of the shadow cure process is of tremendous value since it allows the effects of a variety of process variables to be characterized and understood efficiently and with a reduced number of laboratory experiments. For modeling purposes, it is convenient to consider the active center generation step and the active center migration step separately since these two steps are driven by different fundamental processes and

occur on different timescales. The information gained in the active center generation model will be used as an initial condition in the active center migration analysis.

3.4.1. Active Center Migration Model

The active center concentrations at the end of the illumination step described in the previous section provides the initial conditions for the shadow cure active center diffusion calculations. As illustrated in Figure 3.6, these profiles fall off rapidly and therefore exhibit a sharp gradient and a considerable driving force for diffusion. According to Fick's second law, the diffusion can be related to the concentration profile using the following equation.

$$\frac{\partial C_{ac}(z, t)}{\partial t} = D_{ac} \frac{\partial^2 C_{ac}(z, t)}{\partial z^2} \quad (3.9)$$

Here, $C_{ac}(z, t)$ is the active center initiator molar concentration at depth z and time t and D_{ac} is the diffusion coefficient of the active center in units of length²/time. Figure 3.17 contains active center migration profiles obtained using this equation for the conditions shown previously in Figure 3.6 (the 5 minute active center profile from Figure 3.6 was used as the starting condition for the active center diffusion). Figure 3.17 illustrates that the active center profile broadens and extends deeper into the sample as that shadow cure time is increased due to active center diffusion. The experimentally observed cure heights at each representative time are represented as circles in the figure. These values suggest that a threshold value of the active center concentration is required to fully cure the surrounding monomer, rendering it insoluble in the THF solvent. Analysis of the data reveals that the active center threshold concentration is 0.0013 ± 0.0003 mol/L. This value will be used in further analysis to predict the shadow cure distance.

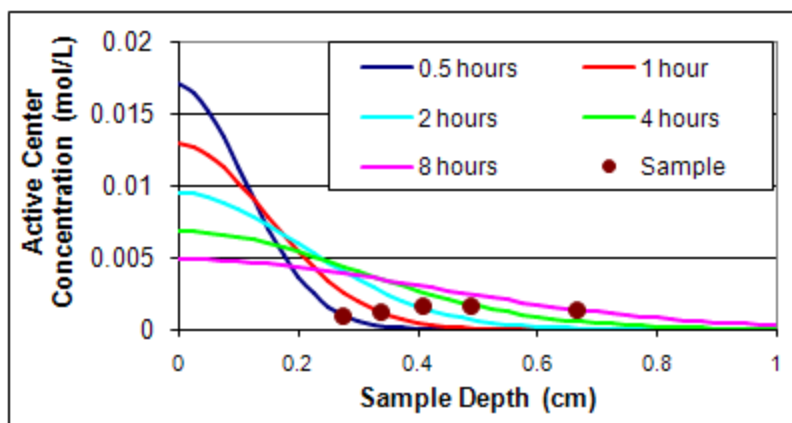


Figure 3.17. Modeled active center spatial profiles during shadow cure. Monomer: CADE, Initiator: 0.5 mol% IPB, Exposure time: 5 min, Exposure Temp.: 25°C, Shadow Cure Temp.: 50°C, Diffusion Coefficient: $9.2 \times 10^{-6} \text{ cm}^2/\text{sec}$

3.4.2. Verification of the Active Center Migration Model

The active center migration was analyzed using the method described above for several different variables including exposure time and temperature. The first variable was exposure time which is one of the easiest variables to control in the laboratory or production settings. In general, the exposure time (for a given initiator concentration and light intensity) determines the number of active centers produced during the illumination. The longer exposure times allow the light to penetrate further into the system due to the photobleaching effect of the initiator. The spatial profile of the active centers created using different exposure times were studied during shadow cure. At each shadow cure time, the depth at which the number of active centers no longer exceeds that threshold value was recorded and shown in Figure 3.18 as the predicted sample height after shadow cure. Figure 3.18 compares both the predicated sample thickness and the experimental value found for an exposure time of three minutes. The predicated sample height typically lies within the experimental values standard deviation value of 0.45mm demonstrating this model can accurately predict the sample thickness due to active center migration for different exposure times.

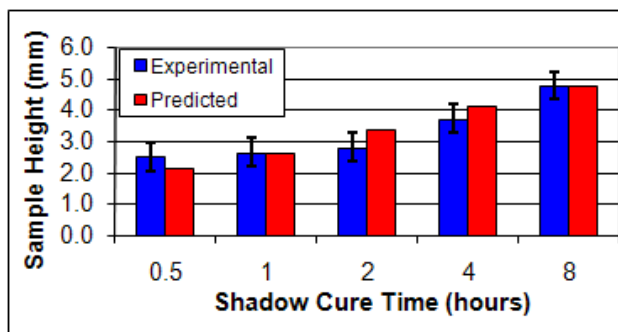


Figure 3.18. Predicted and experimental polymer height for a thick system. Monomer: CADE, Initiator: 0.5mol% IPB, Exposure Time: 3 minutes, Exposure Temperature: 25°C, Shadow Cure Temperature: 50°C, Diffusion Coefficient: $9.2 \times 10^{-6} \text{ cm}^2/\text{sec}$

A second verification study of the model was performed. Figure 3.19 shows both the predicted sample thickness (distance from illuminated surface that still exceed threshold value for polymerization) and the experimental value found for a storage temperature of 40°C. The different temperature value did not change the initial spatial profile but changed the diffusion coefficient. Again, despite the different diffusion coefficient entered, the predicted sample height lies within the experimental values average standard deviation value of 0.45mm. This study further verifies that the model can accurately predict a sample thickness due to active center migration.

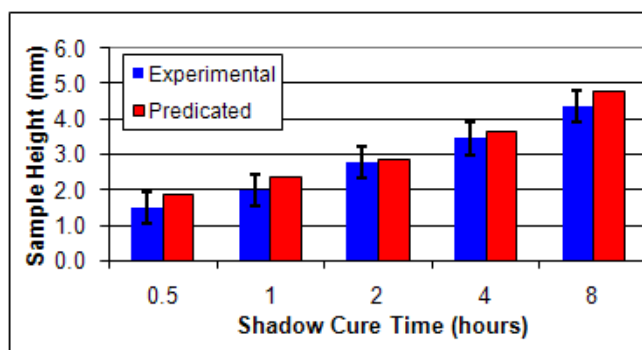


Figure 3.19. Predicted and experimental polymer height for a thick system. Monomer: CADE, Initiator: 0.5mol% IPB, Exposure Time: 3 minutes, Exposure Temperature: 25°C, Shadow Cure Temperature: 40°C, Diffusion Coefficient: $3.0 \times 10^{-6} \text{ cm}^2/\text{sec}$

3.5. Conclusions

In this contribution it is clearly shown that long-lived cationic active centers may lead to shadow cure of unilluminated regions in a thick sample. An analysis based upon the set of fundamental differential equations which govern the evolution of the light intensity gradient and initiator concentration gradient for multi-wavelength illumination was used to model the initial cationic active center profiles. Inspection of these initial profiles revealed that active centers are created only in the first few millimeters of a thick sample and therefore any polymerization past this region must be due to active center migration. A series of experiments were performed to investigate this migration. In these experiments, active centers were produced in the first 0.7 mm of a thick system by illuminating one end for five minutes, and the polymerization progression was monitored up to eight hours. A polymerization front was observed to move from the illuminated region into the shadow region at a rate proportional to the square root of time. The effective shadow cure diffusion coefficient at 50°C was found to be $9.2 \times 10^{-6} \text{ cm}^2/\text{sec}$, and the temperature dependence of the diffusion coefficient was well described by the Arrhenius relationship with an activation energy of 89 kJ/mol. This value is close to the activation energy of propagation for cationic ring-opening polymerizations of oxiranes in highly crosslinked systems. Studies based upon photoinitiator counter-ions of differing size revealed that the system with the larger counter-ion (and therefore a correspondingly higher propagation rate constant) exhibited a significantly higher effective shadow cure diffusion coefficient. An investigation into the photoinitiator concentration revealed that increasing the photoinitiator increasing the active center concentration gradient (leaving the total number active centers constant) between the illuminated and shadow regions therefore driving the active center to migrate though diffusion. Increasing the exposure time will increase the overall number of

active centers while leaving the counter-ion concentration constant. This increase leads to more active centers available to migrate and therefore shadow cure of thick polymer systems. All of the experimental observations are consistent with the hypothesis that the active center mobility responsible for shadow cure arises largely from reactive diffusion. Knowing the driving forces behind shadow cure allows the amount of shadow cure a system exhibits to be predicted using a differential finite element analysis of Fick's second law. This analysis accurately describes the experimental shadow cure. All of these investigations illustrate that the long lived cationic active centers are mobile and have the potential to cure thick polymer systems by migrating from the illuminated regions where they are created into deeper unilluminated regions of the thick sample.

CHAPTER 4: ABILITY OF CATIONIC PHOTOPOLYMERIZATIONS TO CURE

PIGMENTED SYSTEMS

4.1. Introduction

While photopolymerization is well known as the optimal method for obtaining clear coats, it has many problems with curing systems with additives. Additives (typically pigments or fillers) can absorb or reflect the incoming photons which the photoinitiators need to react, hindering the light-induced active center formation especially beneath the surface.¹ This causes the pigmented systems to have incomplete cures or uneven cures. Since these additives are necessary for many applications, a solution to this light attenuation problem must be found.

The long lifetimes and mobility of the cationic active centers were studied to determine their ability to fully cure systems that contain different additives. Two primary pigments along with two weathering agents were investigated. The first pigment, carbon black, is known to be very difficult to photopolymerize due to its absorption across all wavelengths of incoming photons. The second pigment, titanium dioxide (TiO₂), is also very difficult because it reflects incoming photons across all wavelengths. The effect pigments' absorption, and loading has on cationic active center generation and mobility was explored through a number of methods. The effect of the two weathering agents, UV absorbers (UVA) and hindered amine light stabilizers (HALS), were also studied to investigate their effect on the cationic active center mobility.

4.2. Research Method

4.2.1. Materials

The photoinitiator used for the additive studies was (tolycumyl)iodonium tetrakis (pentafluorophenyl) borate (IPB, Secant Chemicals). The monomer 3,4-

epoxycyclohexylmethanyl 3,4-epoxycyclohexanecarboxylate (CDE, Dow Chemical Co.) with 2-butoxymethyl-oxirane (BMO, Hexion Specialty Co.) to aid in the wetting of aluminum q-panels, was used in these investigations into photopolymerizing coatings with additives. Carbon Black (CB, NIPex 35, Degussa via Xerox) with a particle size of ~31 nm was used as the primary pigment. Titanium dioxide (TiO₂, Dupont via Toyota) with a particle size of ~44 nm was used as the primary white pigment filler. The UV light stabilizer studied was benzenepropanoic acid (UVA, Ciba Specialty Chemical Corp.) while the hindered amine light stabilizer investigated was bis (1-octyloxy-2,2,6,6-tetramethyl-4-piperidyl) sebacate (HALS, Ciba Specialty Chemical Corp.).

4.2.2. Experimentation Method

Cationic shadow cure's ability to overcome the light attenuation created by pigments was studied. To perform these experiments, solutions containing 70wt% CDE, 23-29% BMO, 1wt% IPB, and 0-6wt% pigment were created and mixed together for 24 hours under dark conditions. Once the solution was mixed, it was then sprayed onto an aluminum substrate using an airbrush (where the coating thickness average $40\mu\text{m} \pm 15\mu\text{m}$). The coated panels were then illuminated for 5 minutes, using a 200 W Oriel Hg-Xe arc lamp. The irradiance of the lamp was measured to be $\sim 50.0 \text{ mW}/\text{cm}^2$. The photopolymerization was carried out under atmospheric conditions and at room temperature. The exposed panels were stored at room temperature or in an oven at 50°C. After exposure, the system was monitored to determine the time it took to get a tack-free polymerization. Once polymerized, the thickness of the coating was obtained by a micrometer (micro-TRI-gloss μ , BYK Gardner) using eddy current measurements.

4.3. Research Results Using Carbon Black

Carbon black is virtually pure elemental carbon in the form of colloidal particles that is used in a number of applications. The largest application of carbon black is in the rubber industry where it is used as both a filler and a reinforcing agent since its addition improves tensile strength, wear resistance, and heat conductivity. Carbon black is also used in coating applications for its pigmentation, conductivity, and UV protection. This UV protection arises from the fact that carbon black has a high absorbance across all UV and visible light wavelengths.¹ While this absorption is helpful in many applications, it causes a great deal of interference with photopolymerization. Carbon black (1wt%, particle size 31nm) has a high absorptivity of $\sim 27,000 \text{ cm}^{-1}$ in the wavelengths between 297 and 308nm, causing a great deal of competition with the iodonium salt photoinitiator for the incoming photons. This direct competition greatly reduces the number of cationic active centers produced as shown in active center profile created by the active center generation model, Figure 4.1. Even the small addition of 1wt% carbon black reduces the depth at which active centers are created by two orders of magnitude (from $\sim 0.7\text{mm}$ to $\sim 0.003\text{mm}$).

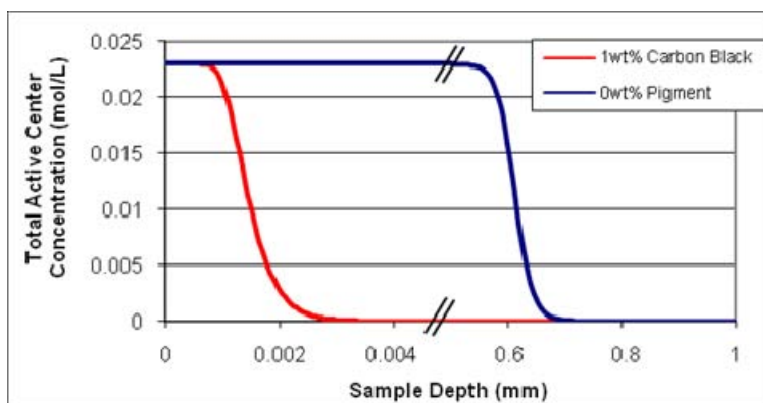


Figure 4.1. Active center concentration profiles modeling effect of carbon black. Monomer: CDE, Initiator: 0.5 mol% IPB, Exposure time: 5 min, Exposure temp.: 25°C, Intensity: 50mW/cm²

As discussed in chapter three, reducing the number of active center reduces the driving force behind their mobility. Using the experimental method described in chapter three reveals that the reduction in the number of active centers available to migrate, reduces driving force behind the active center mobility and therefore reduces the effective shadow cure diffusion coefficient by two orders of magnitude, from $9.2 \times 10^{-6} \text{ cm}^2/\text{sec}$ to $1.4 \times 10^{-7} \text{ cm}^2/\text{sec}$ upon the addition of 1wt% of carbon black. The lower effective shadow cure diffusion coefficient means that while thick systems can be created, it takes a lot longer. For example, the 1wt% sample in Figure 4.2 took approximately two weeks to create.



Figure 4.2. A thick 1wt% carbon black polymer created by shadow cure.

Although this reduction in driving force and active center numbers means thick polymer systems take longer to create, thin polymer systems such as the $\sim 40\mu\text{m}$ coatings described in this chapter's method section can still be efficiently shadow cured. A $40\mu\text{m}$ pigmented coating containing 1wt% carbon black was fully polymerized within the 5 minutes of illumination. This means the active centers produced in the first $3\mu\text{m}$ of the sample, quickly migrated $37\mu\text{m}$. This indicates that while the number of active centers generated in systems pigmented with carbon black is reduced, there are still enough active centers being created to fully polymerize a thin pigmented polymer coating.

4.3.1. Effect of Carbon Black Loading

The addition of pigments to a coating formulation interferes with the absorption of the photoinitiator and ultimately decreases the number of active centers produced. Using the active center generation model, the concentration of active centers throughout the coating depth was calculated for systems pigmented with different weight percents of CB (particle size 31nm) and is shown in Figure 4.3. The addition of even a small amount (1wt%) of pigment drastically reduced the depth in which active centers are produced to $\sim 3.0\mu\text{m}$. As the pigment loading increases, the depths at which cationic active centers are produced further decrease to below $1\mu\text{m}$.

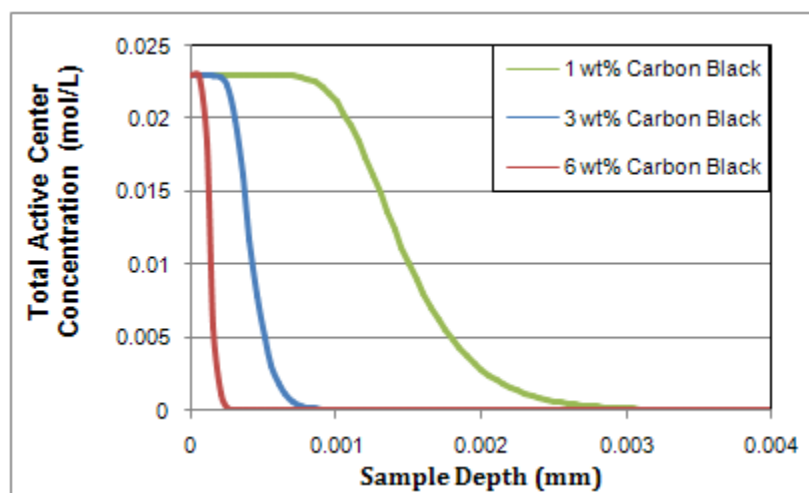


Figure 4.3. Active center concentration profiles for carbon black with different pigment loadings. Monomer: CDE, Initiator: 0.5 mol% IPB, Exposure time: 5 min, Exposure temp.: 25°C , Intensity: $50\text{mW}/\text{cm}^2$

Coatings with these different pigment loadings were applied to aluminum substrates to investigate the effect that different pigment loadings have on the shadow cure of thin systems. The results, summarized in Table 4.1, reveal that despite active centers only being created in the

top few micrometers of the 40 μ m sample, the coating was fully polymerized. The time (after 5 minutes of illumination) to achieve this tack-free polymerization took longer as the pigment loading was increased. This increase in time is due to the reduction of active centers and therefore the driving force behind their migration. The slower migrating active centers take longer to traverse into deeper regions that received no illumination due to carbon black interference.

Pigment Loading	Tack-Free Cure Time
0wt%	0 minutes
1wt%	0 minutes
3wt%	<30 minutes
6wt%	<1 hour

Table 4.1. Time to achieve tack-free cure for systems with 0-6wt% CB pigment loadings.

4.3.2. Effect of Temperature

Temperature was shown in chapter three to have a significant effect on the active centers mobility for thick systems. Experimentally, it was found to have a similar effect on curing thin pigmented coatings. A sample pigmented with 6wt% carbon black took approximately an hour to shadow cure to a tack free coating at room temperature. When a similar sample was stored at 50°C, the migration speed of the active centers was increased so they could easily penetrate and polymerize the deeper unilluminated regions of the sample, thus creating a fully converted tack-free coating faster. By increasing the temperature, the time it took to shadow cure a coating pigmented with 6wt% carbon black was reduce from between a half-hour and an hour to less than a half-hour.

4.3.3. Effect of Exposure Time

It was shown in chapter three that in thick systems as the exposure time of a sample is increased, the extent of shadow cure and cationic active center migration speed is increased. The effect of the exposure time on thin pigmented coatings, shown in Table 4.2, reveals the same trend, namely that increasing the illumination time decreases the time it takes to achieve a tack free cure. At longer illumination times, the total number of active centers is increased which leads to an enhanced driving force for diffusion. Enhancing the driving force behind the cationic active centers mobility enhances the mobility and corresponding extent of shadow cure. The increase in migration speed means the active centers do not need as much time to fully cure coatings with pigments.

Exposure Time	Tack-free Cure Time
1 minute	1.5 hours
2 minutes	<30 minutes
3 minutes	0 minutes
4 minutes	0 minutes
5 minutes	0 minutes

Table 4.2. Time to achieve tack-free cure for 3wt% CB polymer systems illuminated for different durations.

4.4. Experimental Results using Titanium Dioxide

Titanium dioxide is the most widely used white pigment because of its brightness and very high refractive index. This reflection, which is very good for its many applications, hinders the production of active centers by reflecting incoming photons thus preventing the photoinitiators from absorbing them.¹ Using the active center generation model, the active center production for a TiO₂ sample (1wt%, particle size 44nm) was found and placed in Figure

4.4. The active center generation profile without titanium dioxide would produce active centers in depths up to 0.7mm while the addition of 1wt% reduces this to 3.5 μ m. This reduction is still significant though it is not as much as carbon black.

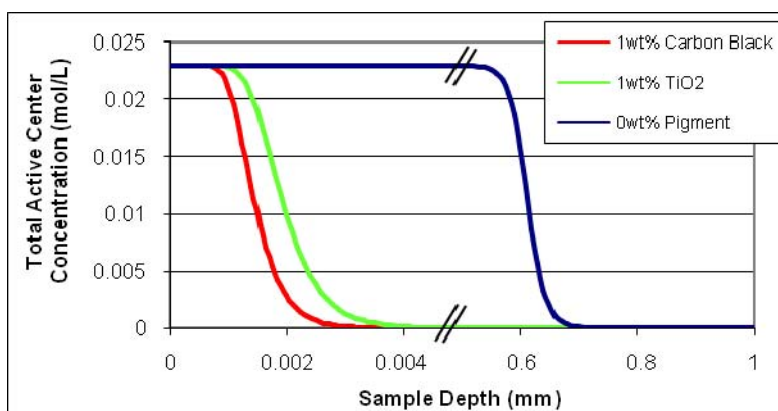


Figure 4.4. Active center concentration profiles modeling effect of TiO₂ as compared to CB and neat systems. Monomer: CDE, Initiator: 0.5 mol% IPB, Exposure time: 5 min, Exposure temp.: 25°C, Intensity: 50mW/cm²

When the cationic photopolymerization ability to cure a system pigmented with TiO₂ was investigated it was found that it has many of the same trends as CB. As shown in Table 4.3, as the TiO₂ pigment loading was increased, the time it took to achieve a tack-free cure also increased. This increase in time arises from the fact that less active centers are being created and therefore the driving force behind their migration is reduced.

Pigment Loading	Tack-free Cure Time
0wt%	0 minutes
1wt%	0 minutes
3wt%	0 minutes
6wt%	<30 minutes

Table 4.3. Time to achieve tack-free cure for systems with 0-6wt% TiO₂ pigment loadings.

The effect of exposure time was also investigated. The results, shown in Table 4.4, again reveal the same trend as the carbon black samples, specifically shortening the illumination time increased the time it took to achieve a tack free cure. Since reducing the exposure times decreases the overall amount of cationic active centers that are produced, the driving force behind their mobility is lessened and their migration speed slowed. The slowing in migration speed means the active centers need more time to fully cure a coating that contains additives.

Exposure Time	Tack-free Cure Time
1 minute	2 hours
2 minutes	1 hour
3 minutes	<30 minutes
4 minutes	<30 minutes
5 minutes	0 minutes

Table 4.4. Time to achieve tack-free cure for 3wt% TiO₂ polymer systems illuminated for different durations.

4.5. Research Results using Other Additives

There are numerous other additives and pigments that could be added into a photopolymerizable coating. Antifoaming agents, conductive particles, expanding fillers, surfactants are just a few.⁵ Two common additives to prevent weathering are UV absorbers (UVAs) and Hindered Amine Light Stabilizers (HALS). These additives have been typically used with coatings to prevent photooxidation of the coating.¹ Photooxidation happens when sunlight and oxygen react with the polymer backbone creating free radicals. These free radicals can cause several chemical reactions in the polymer backbone, which have the net result of changing its chemical composition. Photooxidation can be so pronounced that the polymer coating would be completely destroyed within a few days or weeks if directly exposed to light

without any protection. UVAs prevent photooxidation by absorbing the incoming photons, preventing the light from reacting with the oxygen and polymer backbone to produce free radicals in the coatings. HALS prevents photooxidation by acting as a free radical scavenger, eliminating any free radicals if they are formed.

4.5.1. UV Absorbers

The UVAs directly compete with the iodonium salt photoinitiator for the incoming photons, absorbing the light much like the carbon black pigment does.⁸ However, this UV light absorber has a much higher absorptivity than carbon black ($\sim 500,000 \text{ cm}^{-1}$ compared to the $27,000 \text{ cm}^{-1}$ in the wavelengths between 297 and 308nm). The higher absorptivity means that the extreme competition with the photoinitiator for incoming photons greatly reduces the number of cationic active centers produced, as shown in active center profile created by the active center generation model, Figure 4.5. The addition of 1wt% UVA prevents the active centers from being created past $0.083\mu\text{m}$ into the sample, which is two orders of magnitude less than carbon black ($3\mu\text{m}$ or 0.003mm) and four orders magnitude less than a sample with no additives ($700\mu\text{m}$ or 0.7mm).

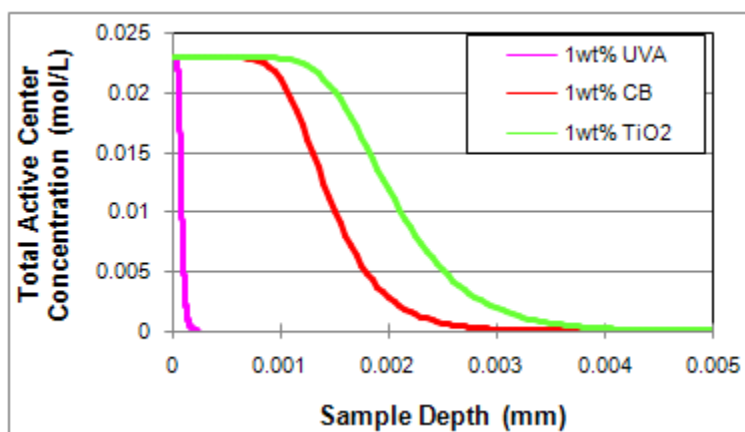


Figure 4.5. Active center concentration profiles modeling effect of UVA in comparison to other additives. Monomer: CDE, Initiator: 0.5 mol% IPB, Exposure time: 5 min, Exposure temp.: 25°C, Intensity: 50mW/cm²

This extreme reduction in active centers considerably slowed the active center migration speed. Using the experimental method described in chapter three reveals that the reduction in driving force behind the active center mobility reduces the effective shadow cure diffusion coefficient from $9.2 \times 10^{-6} \text{ cm}^2/\text{sec}$ to $1.5 \times 10^{-8} \text{ cm}^2/\text{sec}$ upon the addition of 1wt% of UVA. However, this effective shadow cure diffusion was highly unreliable since the shadow cure polymer samples were so thin that recovery of the full sample was extremely difficult.

Even with a reduction of active centers, which slows the active center migration, the 40 μm coating with 1wt% UVA could still be still fully cured within the 5 minutes of illumination. This shows that efficient photopolymerization of coatings with this UV absorber is possible. This allows photopolymerization to be accessible in a number of practical applications in which UVAs must be used.

4.5.2. Hindered Amine Light Stabilizer

The HALS weathering agent does not try to block free radicals from being generated through photooxidation, instead it scavenges the any free radicals that are produced. The absorptivity of this additive is low in comparison to the pigments and UVA ($1,000 \text{ cm}^{-1}$ in the wavelengths between 297 and 308nm). The lower absorptivity allows active centers to be generated up to depths of 36 μm in a sample with 1wt% HALS, as shown in Figure 4.6. The total number of active centers available to migrate is a great deal more than systems pigmented with either CB or TiO_2 but significantly less than a neat system (one with no additives).

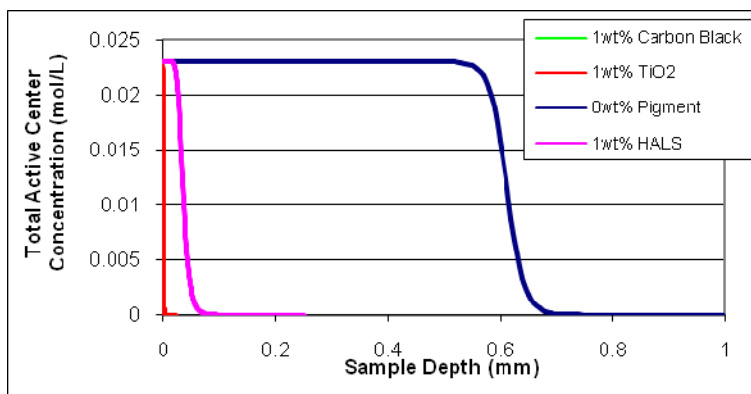


Figure 4.6. Active center concentration profiles modeling effect of HALS in comparison to other additives. Monomer: CDE, Initiator: 0.5 mol% IPB, Exposure time: 5 min, Exposure temp.: 25°C, Intensity: 50mW/cm²

Even though there are many more active centers available to migrate through the system shadow curing the unilluminated depths, no shadow cure was present even after 8 hours of observation in thick monomer systems with 1wt% HALS additive. In a thin coating with 1wt% HALS, the 40 μ m coating took 4 days to fully cure. The impediment of the shadow cure could be caused by the basicity of HALS.⁸ In previous studies, basic electron donors/amines were shown to inhibit the propagation of cation photopolymerization.²¹ The cations are more favorable to reaction with the basic component than to propagation with the monomer, eliminating the polymerization of the system. Therefore, the HALS weathering agent acts as a scavenger to not only the free radicals but the cations as well.

4.6. Conclusions

In this chapter, it is clearly shown that the ability of long-lived cationic active centers to shadow cure can be utilized to fully polymerize pigmented or filled systems overcoming the additive interference. Finite element analysis of the time-evolution of the light intensity gradient revealed that the depth of active center generation can be decreased by two to four orders of magnitude by the presence of the additive (from ~0.7mm to less than a micron). Despite this

reduction in active centers, experimental studies revealed that cationic photopolymerizations can efficiently polymerize pigmented systems by migrating beyond the depth of light penetration. It was found increasing the overall amount of active centers and therefore the driving force behind shadow cure (by changing reaction conditions like the temperature, and exposure time) will increase the cationic active center migration speed and reduce the time it takes to fully cure a coating with additives. The basicity of the additive was shown to be important, since very basic additives (such as HALS) can inhibit the cationic active center polymerization. These studies provide new fundamental information on cationic active center migration through pigmented systems and have important practical implications in a variety of fields and applications where pigments and fillers are necessary.

CHAPTER 5: ABILITY OF CATIONIC PHOTOPOLYMERIZATIONS TO CURE COMPLEX SHAPES

5.1. Introduction

Photopolymerization is well established for coatings on predominately flat, geometrically simple substrates. However, photopolymerization of coatings on complex three dimensional shapes (such as automotive body substrates) are relatively unknown due to problems with oxygen inhibition and shadow regions. These problems which arise from using traditional free radical photopolymerization can be avoided by using cationic photopolymerization.

In this chapter, a unique way to use the ability of long-lived cationic active centers to migrate to photopolymerize complex three-dimensional shapes will be shown. If, as suggested by previous studies,^{7,8,31} the cationic active centers cease to polymerize primarily due to depletion of the monomer rather than chemical termination reactions, they should be particularly long-lived in monomer-free solutions. These photoactivated monomer-free solutions could be used in a two step process to coat a complex shape as shown in Figure 5.1. The first step would be to apply a monomer to the substrate. This would be followed by a second step where previously photogenerated active centers in a monomer-free solution are applied to the substrate. Upon contact with the monomer coated substrate, the previously generated active centers would begin polymerizing the monomer by migrating through the monomer layer. Through this process, the cationic active centers could be applied to complex three dimensional substrates covering the entire surface of the object eliminating shadow regions. If this process was tried with the traditional free radical photopolymerization system, there would only be moments after the free radical active centers are created by illumination that they could be applied before the free radical active centers would terminate themselves by combination or oxygen termination.

Furthermore, only the topmost layer of the coating would be cured before the free radicals terminate themselves, leaving the cure of the deeper regions incomplete.

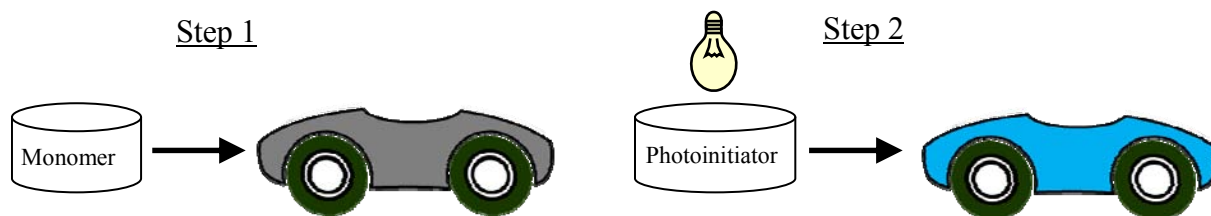


Figure 5.1. Method for using previously generated active centers in two step process.

This method could be modified slightly as shown in Figure 5.2. In this method, the cationic active centers are created in a monomer free solution before any application by illuminating the photoinitiator in an easy lamp configuration. Then the monomer and active center are simultaneously applied to the substrate (mixing in the air and then on the substrate). Here the polymerization may start in the air creating oligomers, but the majority of the polymerization would occur on the substrate. Again, the long active center lifetime will allow them to migrate and cure all the surrounding monomer creating a fully cured coating.

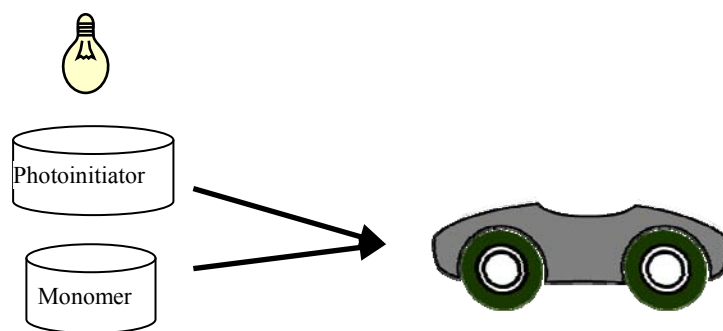


Figure 5.2. Method for using previously generated active centers in single step process.

To ascertain the feasibility of this novel process, experiments were carried out in which the cationic active centers were produced photochemically in a monomer-free solution before adding them to the monomer to be polymerized. The effect storage time (time between illumination and addition to monomer) has on the previously photogenerated active centers was studied as well as the effect of the storage temperature on the monomer-free previous illuminated photoinitiator solution.

5.2. Research Method

5.2.1. Materials

The photoinitiator used for the active center lifetimes in monomer-free solutions experiments was triarylsulfonium hexafluoroantimonate salts 50 wt% in propylene carbonate (THA, Aldrich, Figure 5.3). The cationic monomer used in this research was methyl 3,4-epoxycyclohexanecarboxylate (ECH, Dow Chemical Co., Figure 5.4).

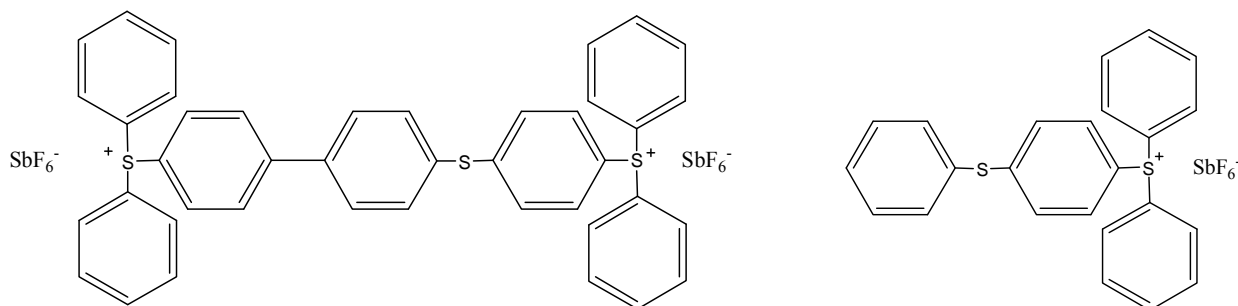


Figure 5.3. Molecular structure of triarylsulfonium hexafluoroantimonate salts (THA).

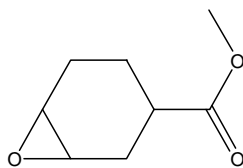


Figure 5.4. Molecular structure of methyl 3,4-epoxycyclohexanecarboxylate.

5.2.2. Methods

The monomer free photoinitiator solution was illuminated, using a 200 W Oriel Hg(Xe) arc lamp, for 10 minutes to ensure complete photolysis of the photoinitiator. The irradiance of the lamp was measured to be 50.0 mW/cm^2 . The photoactivations were carried out under atmospheric conditions and at room temperature. After exposure, the system was maintained at the prescribed temperature for the predetermined storage time in a humidity free environment. After the prescribed storage time, an aliquot of the preactivated photoinitiation solution was taken and added to ~15 mg of monomer. The resulting polymerization occurring upon contact between the active center and monomer was run at 50°C to enhance the speed of the reaction and monitored using a differential scanning calorimeter (DSC). Each polymerization was done in triplicate to ensure the reliability of the results.

5.3. Results and Discussion

5.3.1. Effect of Storage Time on Active Centers Produced in Monomer-free Solution

To characterize the persistence of the active centers after illumination as a function of storage time, the photoinitiator THA was illuminated and stored over a period of 6 weeks at 25°C . At several times during this period, the active centers reactivity was measured using the methods described above to determine if the active centers had undergone any termination. The polymerization rate profiles for each time periods remained essentially the same despite the active centers being generated days before as shown by two representative samples in Figure 5.5.

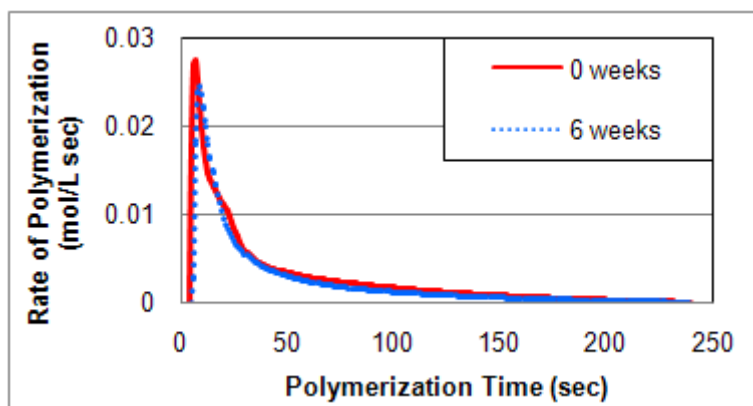


Figure 5.5. Polymerization rate profiles produced using previously photogenerated cationic active centers for two different storage times.

The active center reactivity for each individual storage time is shown in Figure 5.6 by plotting of the maximum polymerization rate observed upon addition of the active center solution to the monomer (normalized by the rate immediately after illumination) as a function of the storage time (which ranged from 1 to 6 weeks). The observed polymerization rates remain constant within the standard deviations, showing that the polymerization rate is independent of the storage time. This indicates that the active centers do not lose reactivity (terminate) during storage and photogeneration of active centers in monomer-free solutions prior to applications is possible.

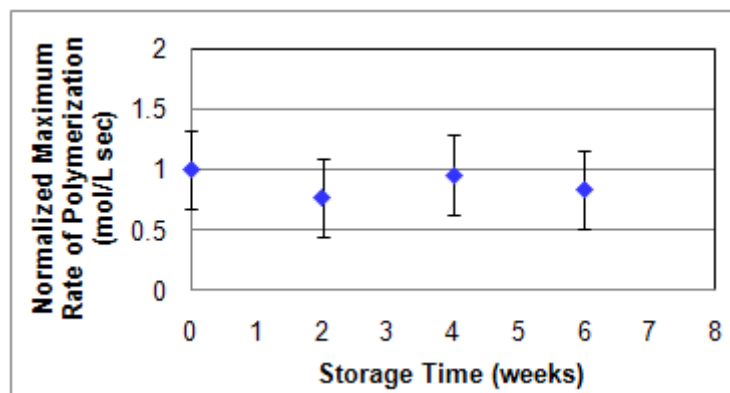


Figure 5.6. Normalized maximum rate of polymerization by previously photogenerated cationic active centers over storage time.

5.3.2. Effect of Storage Temperature on Active Centers Produced in Monomer-free Solution

The robustness of the previously generated active centers when stored at different temperatures was investigated. The results of the photoinitiator THA being illuminated and stored over a period of 6 weeks at 50°C are shown in Figure 5.7. Comparing the data for the two different storage temperatures (25°C and 50°C) reveals the normalized maximum polymerization rate is the same (within the standard deviation of the experiment) for both storage temperatures for up to 6 weeks of storage. These results show that the active center reactivity is not degraded by temperatures up to 50°C indicating the previously photogenerated active centers are stable with time and temperature. This temperature stability will be very useful when apply this novel method in an large-scale industrial setting where the temperature can not be control as easily.

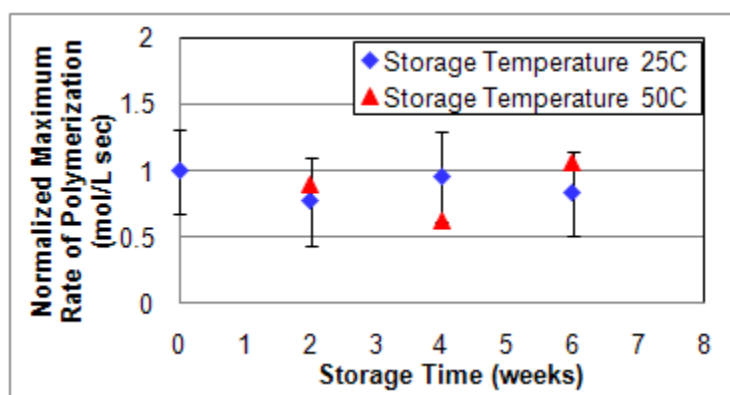


Figure 5.7. Normalized maximum rate of polymerization by previously generate cationic active centers dependence on storage time for two different temperatures.

5.4. Conclusions

In this chapter, it is clearly shown that cationic polymerization can occur by the addition of previously photogenerated active centers created by the illuminated of photoinitiators in monomer-free solutions. These previously photogenerated active centers solutions can be stored

up to six weeks at temperature up to 50°C without any loss of reactivity. This novel method of using previously photogenerated active centers in monomer-free solution to cure complex shapes could have many important applications in the polymer coating field.

CHAPTER 6: CREATING SEQUENTIAL STAGE CURABLE POLYMERS WITH CATIONIC PHOTOPOLYMERIZATIONS

6.1. Introduction

The long lived active centers of cationic photopolymerization can be used to create a unique system when used in conjunction with free radical photopolymerization. This hybrid free radical/cationic photopolymerization system has received considerable attention in recent years. One motivation for investigating hybrid reactions has been to develop a system which overcomes the limitations of the individual reactions. For example, in hybrid photopolymerizations of acrylates and epoxides, Christian Decker and collaborators demonstrated that the oxygen sensitivity of the acrylate was reduced while its ultimate conversion was enhanced.^{7,8} Similar trends were revealed for many other hybrid monomer combinations (acrylate/vinyl ether, vinyl ether/ester, etc).^{7,10} Hybrid photopolymerization has also been investigated as a means to create a variety of novel polymers, including interpenetrating polymer networks (IPNs),^{7, 44} block or grafted copolymer networks,^{11,13} or crosslinked hybrid polymer network.¹²

In this chapter, a relatively new aspect of hybrid photopolymerizations will be investigated: the creation of a sequential stage curable material in which the reaction system exhibits several discrete stages, each with its own set of unique properties. This feature could be useful in a variety of applications in which distinct flowable and shapeable stages are desired before the final rigid polymer is formed. In this contribution, control over the timing of the individual stages through resin formulations and a new photoinitiation formulation will be explored.

6.2. Background of Sequential Stage Curable Hybrid Systems

Sequential, stage-curable hybrid photopolymerizations generally exhibit three distinct states, with either a free radical or a cationic polymerization accompanying the transitions between states, as illustrated in Figure 6.1. The first stage consists of the unreacted monomer mixture; at this time, the system is a relatively low viscosity liquid that may readily flow into small crevices or cracks. The transition from the first stage to the second stage may be driven by either a free radical polymerization (for example, many acrylate/epoxide systems) or a cationic polymerization (for example, most vinyl ether/acrylate hybrid systems). In either case, the first polymerization reaction results in a marked change in the physical properties of the system which undergoes a transition from a relatively low viscosity liquid to a high viscosity shapeable putty. Once the first polymerization is complete the system is in stage 2. The second polymerization (free radical or cationic, opposite that of the first stage) transitions the hybrid system from the 2nd stage into the third and final stage. Again this stage usually has a marked change in the physical properties of the system. The system transforms from the stage 2, a high viscosity shapeable putty to a solid rigid polymer, stage 3.

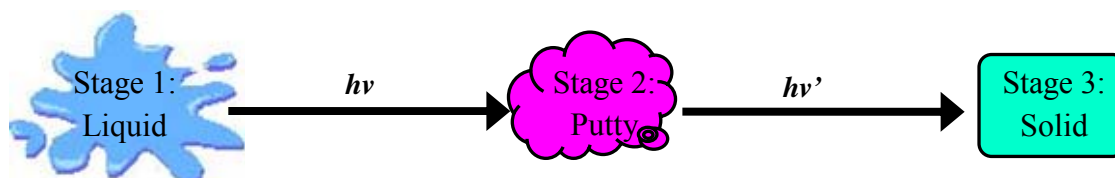


Figure 6.1. The development of the sequential stages in a free radical/cationic hybrid system.

One method for controlling the timing and order of the sequential stages of the hybrid free radical/cationic monomer system is through physically controlling the system. The physical

control comes from having the different monomers initiated at different wavelengths ranges as shown in Figure 6.1. By switching the irradiation source or removing a filter the different monomers can be initiated at any desired time or order. Decker used this physical control to control the stages in a methacrylate/acrylate hybrid system.³ The methacrylate was first polymerized using only the wavelength at 365 nm. After the desired time, the epoxide portion of the reaction was polymerized using the full emission of a mercury xenon arc lamp. Physically controlling the hybrid systems in this way allows for excellent temporal control. The order and sequence of the system can easily be varied. However, in some applications, such as pressure sensitive adhesives, it may not be practical or possible to illuminate a sample twice. For these cases a second control method must be applied.

The second method is to chemically control the sequential stages in a stage curable hybrid free radical/cationic system different stages by adjusting the photoinitiator components or concentrations. This chemical control can be achieved in several ways. The first is using two separate initiators (one a free radical initiator, the other cationic) that absorb the same wavelength. Stansbury *et al.* used this method and found by varying the concentrations of the photoinitiators, the order of the stages in a methacrylates/vinyl ether could be interchanged allowing either the methacrylates or vinyl ether to be polymerized first.⁴⁴ Using separate initiators with a single wavelength eliminates the need to illuminate a sample multiple times to create the stages, simplifying the process. However, the photoinitiators chosen cannot interfere with the other polymerization process since such interference can lead to incomplete cures.

An alternative to using separate initiators to achieve chemical control over the sequential stages was developed by Oxman *et al.* for a methacrylates/cycloepoxide system.^{21,45,46} To initiate and control the system, a three component photoinitiation system was used. This system,

consisting of a photosensitizer (the light absorbing moiety), an electron donor (typically an amine) and an iodonium salt, generated both free radicals and cations from a single initiator system by a series of electron transfer and proton transfer reactions. The basicity of the electron donor was found to have a significant effect of the timing of the epoxide reaction (second stage). It was found that the onset of the second stage could be lengthen or shorten depending on the basicity and concentration of the electron donor. This shows that single photoinitiation systems that generate both free radical and cations are a viable alternative to systems in which separate free radical and cationic photoinitiator are used.

6.3. Research Methods

The monomers used in this study include a cycloaliphatic diepoxide (3,4-epoxycyclohexylmethanyl 3,4-epoxycyclohexanecarboxylate, ERL 4221, available from Dow Chemical Co.) and a hexafunctional acrylate oligomer (Ebecryl 830 available from UCB Chemicals). Polytetrahydrofuran diol (Aldrich) was added to each monomer solution to enhance the cationic rate of the polymerization. The hybrid photopolymerizations were initiated by two different photoinitiation schemes. The first photoinitiation system, used in the monomer control studies, was a visible three-component photoinitiation system containing camphorquinone (CQ, Hampshire Chemical Corp.) as the photosensitizer, ethyl-4-dimethylaminobenzoate (EDMAB, Aldrich) as the electron donor, and diaryliodonium hexafluoroantimonate (DPI, CD1012 available from Sartomer Chemical Co.) as the iodonium salt. Both the hybrid and neat monomer systems were initiated with $3.0 \times 10^{-5} \text{ mol/g stock}$ of camphorquinone (stock solution contains both monomer plus polytetrahydrofuran diol), $2.5 \times 10^{-6} \text{ mol/g stock}$ of ethyl-4-dimethyl-aminobenzoate, and $2.0 \times 10^{-6} \text{ mol/g stock}$ of diaryliodonium hexafluoroantimonate. A second photoinitiation system containing Bis (2,4,6 – trimethylbenzoyl)-phenylphosphineoxide, (BAPO, Irgacure 819,

available from CIBA), (Irgacure 369, from CIBA) and DPI was also studied to see its effect on hybrid photoinitiation in the photoinitiation control studies. Either ethyl-4-dimethylaminobenzoate (EDMAB, Aldrich) or 4-tert-butyl-N,N-dimethylaniline (TDMAB, Aldrich), was added to this photoinitiation system to test how their basicity affects the control over the timing of the stages.

The photopolymerization reactions were monitored using a Perkin-Elmer DSC-7 modified in-house for photo-experiments. The light source was a 200 W Oriel hg(Xe) arc lamp. The output of the lamp was passed through a 400 nm bandpass filter and water filter to eliminate ultraviolet and infrared light from reaching the sample. The filtered light intensity was found to be $\sim 45 \text{ mW/cm}^2$ as measured by graphite disc absorption. The reaction chamber was sealed with a quartz cover and purged with nitrogen. The lamp was turned on 30 seconds after the DSC began recording the heat flow data for each sample. The heat flow data collected by the DSC was converted into the rate of polymerization and conversion using the heat of polymerization, which was estimated as 78 kJ/mol for each acrylate bond and 97 kJ/mol for each epoxide bond.

6.4. Research Results

6.4.1. Control of Sequential Stage Curable Hybrid Systems through Monomer Selection

The stages of a sequential stage curable hybrid system can be controlled through the selected monomers composition of the resin systems. The order and timing of the stages depends on a number of factors including monomer structure (the typical trends for induction times of several main types of monomers are shown schematically in Figure 6.2), and monomer concentrations. Through careful manipulation of these factors, the induction times and order of the different monomers can be controlled which therefore controls the sequence of the stages.

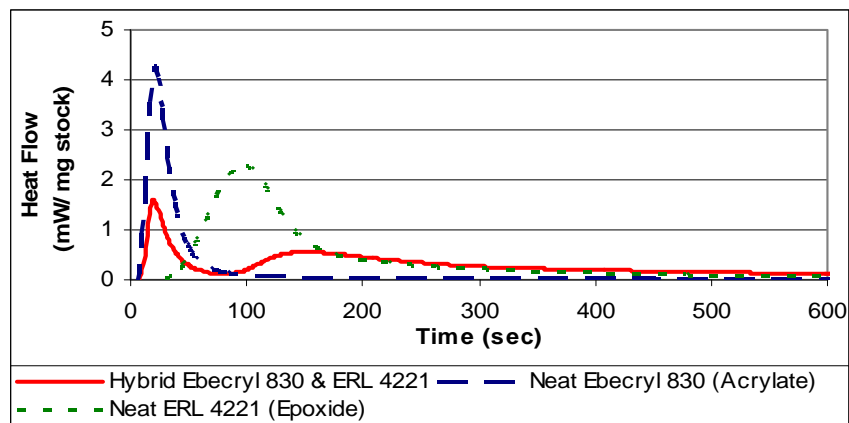


Figure 6.3. Heat profiles comparing the 20% acrylate / 80% epoxide hybrid photopolymerization to neat acrylate and epoxide photopolymerizations.

To investigate whether this polymerization rate reduction could be attributed entirely to the dilution effect by the second monomer, the data was reanalyzed by plotting the heat flow per mg of the monomer that is polymerizing (instead of the heat flow per mg of total solution in the system) in Figure 6.4. The reaction profiles for the neat monomer systems are obtained simply by dividing the heat flow by the initial monomer mass, while the reaction profile for the hybrid system is divided into two regimes. In the first regime, which corresponds to the time from 0 to 108 seconds, the heat flow is divided by the initial mass of acrylate monomer since this is the only monomer that is reacting. Similarly, in the second regime (time after 108 seconds) the heat flow is normalized by the initial mass of the epoxide monomer. Figure 6.4 shows that the acrylate portion of the hybrid system (solid line, first peak) has the same profile as its corresponding neat system (large dashed line), thereby confirming that the reduction in polymerization rate of the hybrid polymerization system can be attributed entirely to the dilution of the acrylate monomer by the presence of the epoxide (there is no evidence of any other interactions).

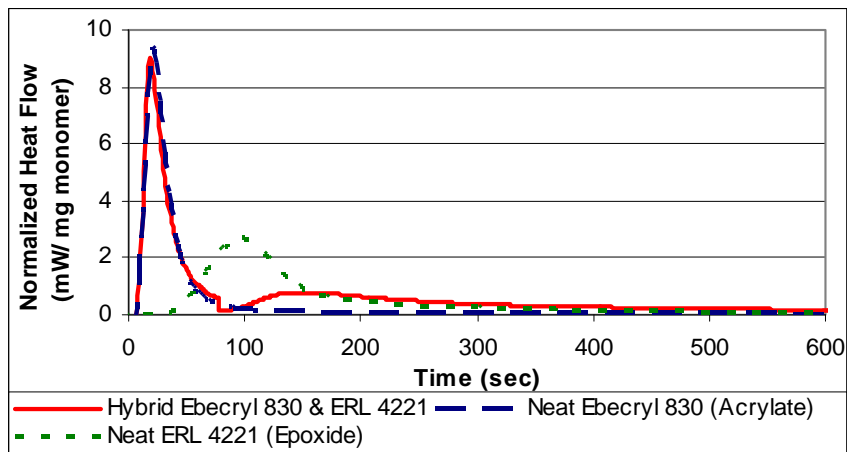


Figure 6.4. Normalized heat profiles comparing the 20% acrylate / 80% epoxide hybrid photopolymerization to neat acrylate and epoxide photopolymerizations.

Figure 6.4, also illustrates some interesting trends in the cationic portion of the hybrid polymerization (solid curve) when compared to its corresponding neat epoxide system (small dashed line). In contrast to the free radical portion, there is clearly a longer induction time before the reaction is perceptible (~ 108 seconds for the hybrid case and ~38 seconds for the neat epoxide), and a marked decrease in the heat flow per milligram of epoxide monomer. The figure illustrates conclusively that these trends in the cationic portion of the hybrid system cannot be entirely attributed to a dilution effect and there are other interactions present.

To investigate this interference further, the normalized heat flow data was transformed into polymerization rate profiles as a function of time (Figure 6.5) using the equation 6.1.

$$R_p (\text{mol} / \text{Ls}) = \frac{\Delta H (W / g) * \rho (g / L)}{\Delta H_p (J / \text{mol})} \quad (6.1)$$

Where R_p in the rate of polymerization, ΔH in the heat observed, ρ is the density, ΔH_p is the standard heat of polymerization. This transformation again illustrates that the reaction profile for the acrylate portion of the hybrid photopolymerization (solid line) system essentially matches that of the neat acrylate system (large dashed line). The polymerization rate when the 25% of the

acrylate is converted is $0.03117 \text{ mol/L-sec}$ for the neat acrylate system. This is comparable to the $0.02753 \text{ mol/L-sec}$ polymerization rate for the acrylate portion of the hybrid system, with a variation of only $\pm 0.0036 \text{ mol/L-sec}$.

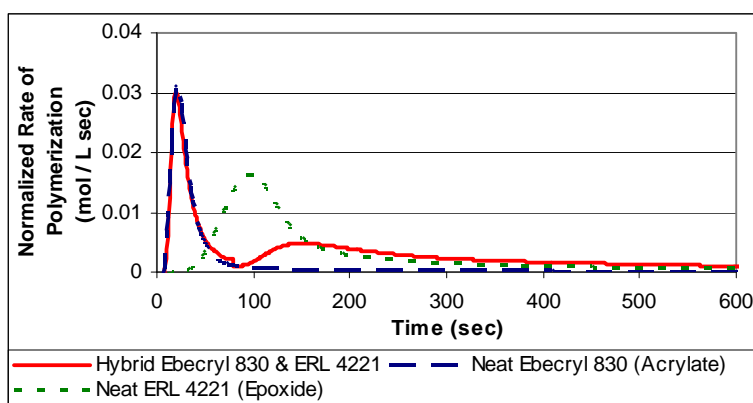


Figure 6.5. Rate of polymerization profiles comparing the 20% acrylate / 80% epoxide hybrid photopolymerization to neat acrylate and epoxide photopolymerizations.

While the hexafuntional acrylate portion of the hybrid photopolymerization system only demonstrates a dilution effect, Figures 6.4 and 6.5 show the cycloaliphatic epoxide portion of the hybrid system is being affected by something beyond dilution. As can be seen above in Figure 6.5, the rate of polymerization for the cycloaliphatic epoxide portion (solid line, second peak) is greatly reduced and the polymerization time is delayed when compared to the neat epoxide system (small dashed line). The rate of polymerization at 10% epoxide conversion is reduced from $0.01605 \text{ mol/L-sec}$ for the neat system to $0.00370 \text{ mol/L-sec}$ for the cycloaliphatic epoxide portion of the hybrid photopolymerization. This is well outside the standard deviation of $0.00131 \text{ mol/L-sec}$ for the epoxide system. The induction time of the epoxide cationic reaction was delayed fifty seconds, from 56 sec. (neat system) to 106 sec. (hybrid photopolymerization

system), which is greatly outside the standard deviation of 11 sec. for the induction time of the cycloaliphatic epoxide.

This reduction of polymerization rates and induction times of the epoxide portion of the hybrid photopolymerization likely arises from the presence of the highly crosslinked acrylate network which will reduce the mobility in the system. Because the acrylate portion of the system is polymerized first, the system becomes highly viscous due to the highly crosslinked acrylate chains. This decreases the mobility of the cationic active centers, thus delaying the induction time and causing the epoxide portion of the hybrid system's rate of polymerization profile to reduce and become more spread out.

If the postulate that the polymerized hexafunctional acrylate is slowing the cationic active centers mobility is correct, then by increasing the ratio of acrylate to epoxide in the hybrid system, the rate of polymerization for the epoxide portion of the hybrid system should continue to decrease and the induction times become more delayed. Figure 6.6 illustrates exactly this trend. The figure shows the normalized polymerization rate profiles as the ratio of hexafunctional acrylate oligomer to cycloaliphatic epoxide monomer is varied. The polymerization rate of the acrylate portion of the hybrid system, seen in Figure 6.6, remains essentially the same (within experimental error), just as in the previous study comparing the 20% acrylate / 80% epoxide hybrid photopolymerization to the neat systems. The epoxide portion of the hybrid photopolymerization system, shown in Figure 6.6, shows a delay in the induction time and a reduction in the polymerization rate as the amount of acrylate in the system was increased.

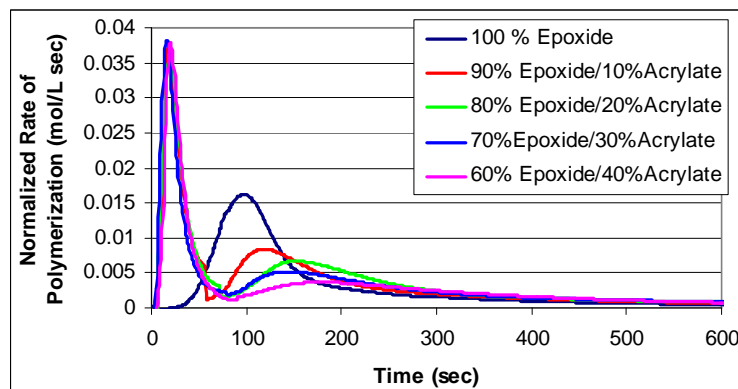


Figure 6.6. Rate profiles showing the effect of epoxide/acrylate ratios has on the photopolymerizations and therefore the sequential stages of the hybrid system.

The delay of induction times that vitrification causes were plotted in Figure 6.7. Figure 6.7 shows that as the ratio of epoxide to acrylate decreases, the induction time of the cationic reaction in the hybrid polymerization will be more and more delayed. Furthermore, it shows that the timing between the stages can be controlled through the monomer selections.

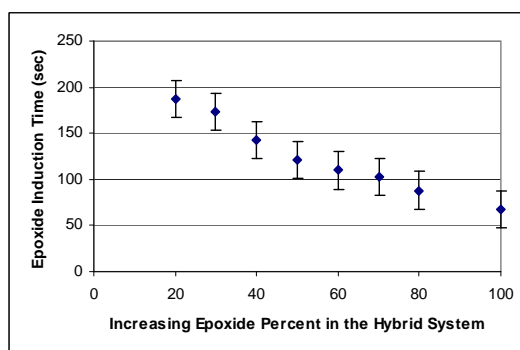


Figure 6.7. Cycloaliphatic epoxide induction times showing the effect that the percent of cycloaliphatic epoxide in the monomer system has on hybrid photopolymerization kinetics.

6.4.2. Control of Sequential Stages through Free Radical/Iodonium Salt Photoinitiation System

Due to their low reduction potential, iodonium salts are excellent electron acceptors, and may oxidize many compounds that contain unpaired electrons, including propagating polymer

radicals. For this reason, a combination of a carefully selected free radical initiator and an iodonium salt could be used to initiate hybrid radical/cationic polymerizations and create a sequential stage curable hybrid system. In this reaction mechanism, shown in Figure 6.8, free radicals are created by photolysis of the radical initiator, and propagate with the acrylate monomer. A fraction of the propagating radicals encounter the iodonium salt which will oxidize the free radical creating a new non-polymerizing free radical and a cation on the propagating polymer chain (which may expel a proton to initiate a cationic polymerizations).

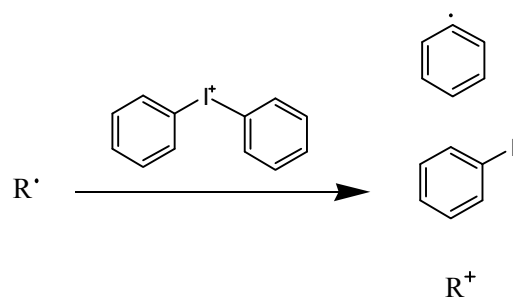


Figure 6.8. Initiation scheme of free radical initiator/iodonium salt hybrid photoinitiators.

A free radical initiator/iodonium salt photoinitiation system based upon BAPO and DPI was investigated for its potential in creating a sequential stage-curable hybrid photopolymerizations. The experimental results summarized in Table 6.1 illustrate that, as the sole component in the photoinitiation system, BAPO (0.5wt%) resulted in a conversion of 83% of the acrylate bonds in a monofunctional acrylate/diepoxide monomer mixture, while no reaction of the diepoxide monomer was observed. In contrast, control experiments performed using DPI (1.5wt%) as the sole photoinitiator component yielded no polymerization of either the acrylate or the epoxide since wavelengths below 400 nm were removed using a bandpass filter, and the DPI exhibits negligible absorbance above 400 nm. Experiments conducted using a photoinitiator

system containing both BAPO (0.5 wt.%) and DPI (1.5 wt.%) revealed that both the free radical and the cationic polymerizations were indeed initiated in a stage curable manner. The free radical polymerization began immediately upon illumination, while the induction time for the cationic polymerization was approximately 230 seconds (greater than 20 percent conversion was noted when the experiment was stopped after 30 minutes). The long lifetimes of the active center continued to cure at a slow rate (too slow for the DSC to observe) and the final hybrid polymerized polymers were glassy and hard to the touch. These results show that the free radical/iodonium salt initiation system was indeed effective in initiating both polymerization mechanisms.

Initiation System	Acrylate Max. Rate of Polymerization (mol/L sec)	Acrylate Total Conversion	Epoxide Max. Rate of Polymerization (mol/L sec)	Epoxide Total Conversion	Epoxide Induction Time (sec)
BAPO	0.0194	83%	-	-	-
DPI	-	-	-	-	-
BAPO + DPI	0.0223	83%	0.0007	>20%	234
BAPO +DPI + EDMAB	0.0244	83%	0.0009	>23%	225
BAPO +DPI + TBDMA	0.0182	81%	-	-	>30 minutes

Table 6.1. Comparison of different photoinitiation systems used in the polymerization of a 20% monoacrylate / 80% diepoxide hybrid monomer solution

Even with the BAPO/DPI photoinitiator system initiating both the free radical and epoxide monomers, in order for the system to be a viable alternative for creating a sequential stage curable hybrid system control over the stages must be achieved. In a previous study, Oxman *et al.* prove that the basicity of an amine in the photoinitiation systems can control the onset of the third stage.²¹ The last two rows of Table 6.1 illustrate the impact of the addition of a

third (amine) component to this photoinitiator system. As seen in table 6.1 above, the less basic EDMAB ($pK_b \sim 11$) slightly enhanced the cationic portion of the polymerization while the more basic TBDMA ($pK_b \sim 8$) inhibited the cationic polymerization. These results suggest through changing the basicity, the induction time of the 3rd stage could be shortened by adding less basic amines (such as EDMAB) or lengthens by adding very basic amines (such as TBDMA) while having no affect on the induction of the free radical 2nd stage.

6.5. Conclusions

Sequential stage curable systems (with three distinct stages) are only possible due to the cationic active center lifetimes being long enough to support length between the stages. The temporal control of the discrete stages in sequential stage curable material can be achieved through a number of methods. Once such control method uses the composition of the monomer resin. The presence of the highly crosslinked acrylate network reduces the mobility of the cationic active center delaying the start of the polymerization and the establishment of the 3rd stage. Increasing the degree of the free radical network (by increasing the amount of free radical monomer in the system) further slows the cationic active centers mobility and delays the induction of the cationic polymerization creating a method for temporal control of the stage timing. Temporal control over the sequential stages of the hybrid material can also be achieved using a free radical/iodonium salt photoinitiator with the addition of an amine. The basicity of the added amine will determine how long the induction of the third stage is delayed. The temporal control and unique properties of the distinct stages make sequential, stage-curable hybrid photopolymerization systems attractive for a wide variety of applications. While the applications have yet to be developed, there are a number of intriguing possibilities, including; medical systems, rapid prototyping resins, advanced coatings and adhesives.

CHAPTER 7: ABILITY OF CATIONIC PHOTOPOLYMERIZATIONS TO ACHIEVE
TEMPORAL CONTROL OF POLYMERIZATION THROUGH A REVERSIBLE WATER
INHIBITION

7.1. Introduction

While photoinitiated cationic polymerizations offer many important advantages for industrial applications, one potential disadvantage of cationic active centers is their sensitivity to moisture. Typically, the addition of water results in inhibition or reduction of the cationic polymerization. However, the chemistry behind this sensitivity to moisture is very complex and relies on a number of factors such as the type and structure of monomer or the concentration of water.

While this sensitivity is usually view as a negative, the moisture sensitivity of the cationic active centers might be used to temporally control the cationic photopolymerization. This chapter will explore this method of temporal control using vinyl ethers that do not contain hydroxyl end groups. The effect of the atmospheric moisture concentration on the active center will be investigated along with the effect of varying this moisture content *in situ*.

7.2. Background on Cationic Photopolymerization
Water Sensitivity

Recently, a number of authors have investigated the effect of moisture on cationic photopolymerizations.^{47- 50} For example, Lin and Stansbury used real time infrared spectroscopy (FT-IR) to investigate cationic polymerizations of vinyl ethers containing water added directly to the formulation, and found that the monomer structure had an important impact on the inhibition mechanism. For monomers containing hydroxyl groups, increasing amounts of water resulted in large reductions of polymerization rate but similar induction times and final conversions.⁴⁷ It was concluded that the hydroxyl-terminated vinyl ethers undergo an unusual self polyaddition in

which the hydroxyl group will react with the vinyloxy functionality of another monomer resulting in formation of polyacetals. Water slows this polyacetal formation but does not have significant affect on the final polymer properties.

The water inhibition for cationic photopolymerizations of vinyl ether monomers which do not contain hydroxyl groups has been recently studied by both Lin and Stansbury⁴⁷ and Crivello *et al.*⁴⁸ Lin and Stansbury reported the induction times of the polymerization increase with increasing water content, but the overall polymerization rate and final conversion remain unaffected. The authors concluded that for these monomers, water will react with the cationic active center in a chain transfer reaction producing another active center, as shown in Figure 7.1A. The hydroxyl formed in this reaction may carry out a second chain transfer reaction to consume a second propagating chain and produce a second proton. In both of these chain transfer reactions, the resulting proton is much more reactive to water than vinyl ether monomers. The proton will participate in the reaction, shown in Figure 7.1B, to produce a hydronium ion that is not active for initiation of the monomer, therefore decreasing the active center concentration.⁴⁷ Crivello *et al.* investigated cationic photopolymerizations of vinyl ethers containing water introduced from the atmosphere rather than being mixed into the original formulation.⁴⁸ Using optical pyrometry, the authors again concluded that cationic active centers will preferentially react with water until water is depleted from the system and only then will the remaining cationic active centers polymerize the monomer.

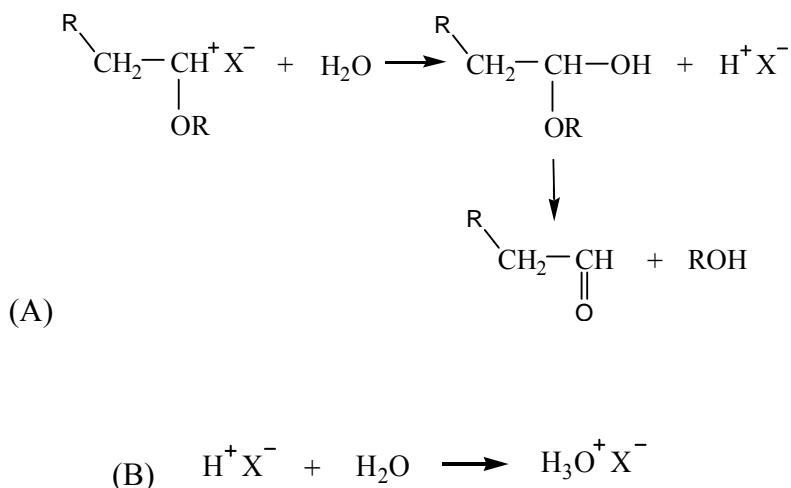


Figure 7.1. Reactions of water and cationic active centers in vinyl ether polymerization systems without hydroxyl end groups

7.3. Research Methods

The research experiments were designed and carried out by Ruiping Huang who at the time of the experiments was a post-doctoral member of the Scranton research group. He left the Scranton research group before any analysis of these experiments could be performed.

7.3.1. Materials

The monomer Dodecyl Vinyl Ether (DVE), was purchased from Sigma Chemical. This monomer, whose chemical structure is shown in Figure 7.2, was selected because it is a mono(vinyl ether) with a low vapor pressure that contains no hydroxyl groups. An iodonium triflate (IT) salt supplied by Dow Corning is shown in Figure 7.3 and was used as the cationic photoinitiator at concentrations of 0.15 mol%.

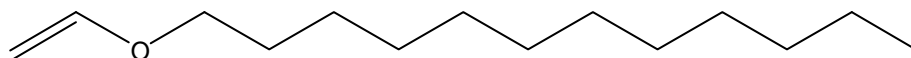


Figure 7.2. Molecular structure of dodecyl vinyl ether (DVE).

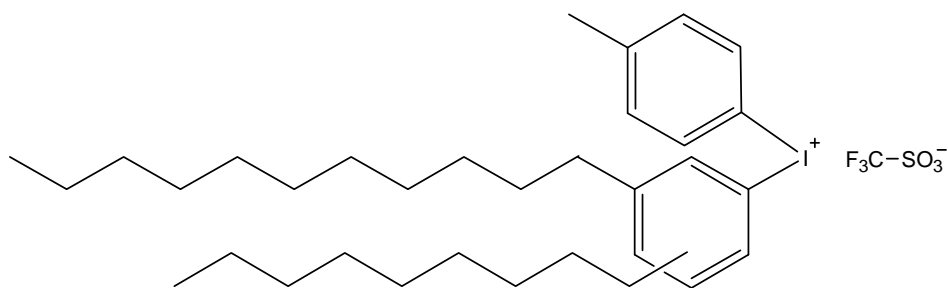


Figure 7.3. Molecular structure of iodonium triflate salt (IT)

7.3.2. Methods

The reaction chamber was constructed out of glass with the exception of the top surface, which was quartz to allow UV illumination from above. The bottom glass surface was cooled with circulated water to keep the temperature constant (23°C). A type 61 IR Card (3M Corp.) was used to maintain a well-defined film thickness of 30 to 50 microns. Raman scattering was induced with 200 mw of 514.5 nm radiation from a Coherent Innova 70 argon ion laser. The Raman probe beam was focused and entered the glass bottom at large angle (> 70 degree) to increase the light path in the mixture. A low pressure Hg lamp (Oriel, Model 6034) was used as UV light source. To test the effects of moisture, the chamber was purged with nitrogen (ranging from dry to water-saturated) at a rate of at least 0.5 L/minute. The Raman signal was collected using a Spex 1877 Triplemate monochromator, and the light was focused onto a liquid-nitrogen-cooled CCD detector (EG&G Princeton Applied Research Model 1530C/CUV). The data were analyzed with an OMA 4000 detector controller and software. The monomer conversion was determined by monitoring the peak area of the doublet at 1630 cm^{-1} which arises from the double bond and represented the concentration of non-polymerized vinyl. The peak area at 1460 cm^{-1} which arises from the wagging and bending of the ethyl ether carbon-hydrogen bonds was used as internal standard.

7.4. Results and Discussion

7.4.1. Effect of Moisture Concentration: Water Inhibition

The effect of atmospheric moisture on the photopolymerization of DVE is illustrated in Figure 7.4 which shows the DVE conversion for three different nitrogen atmospheres: dried nitrogen (0% relative saturation), 50% relative saturation, and 100% relative saturation. The figure illustrates that the polymerization proceeds rapidly with no induction time under dry conditions (with 50% converted in 5 seconds), and is completely inhibited when the polymerization is attempted in a nitrogen atmosphere that is saturated with water vapor (no conversion was noted even after 150 seconds of illumination). For the system polymerized in a 50% saturated nitrogen atmosphere, an induction time of 10 seconds is observed during which the conversion remains essentially zero. At the end of this induction time, the reaction proceeds at a slower rate than the dry system. The effects of the atmospheric relative saturation on the induction time and the time to reach 50% conversion are summarized by the data in Table 7.1. Since these reactions are carried out in films that are exposed to nitrogen atmospheres of constant humidity, water is able to enter the system from the atmosphere. Therefore, water that is consumed by the reaction shown in Figure 1b can be replenished from the atmosphere, and in the case of 100% relative saturation, this prevents the polymerization from taking place. For the case of 50% relative saturation, the shape of the polymerization profile depends upon both the initially dissolved water and the additional water that enters from the atmosphere.

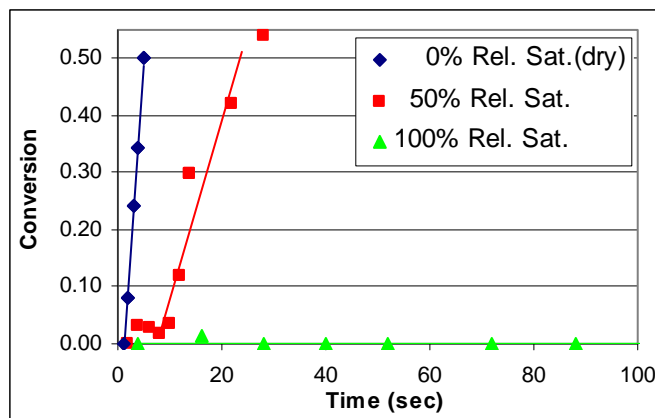


Figure 7.4. Conversion versus time for cationic photopolymerizations of DVE in nitrogen atmospheres of 0%, 50%, and 100% relative saturation.

Atmospheric Relative Saturation	Induction time (seconds)	Time to reach 50% conversion
0%	0 sec	5 sec
50%	10 sec	~25 sec
100%	∞	∞

Table 7.1. Induction time and time to reach 50% conversion for cationic photopolymerizations in nitrogen atmospheres of 0%, 50%, and 100% relative saturation.

7.4.2. Varying Moisture Concentration in Situ: Reversing the Water Inhibitor

In this study, the reversibility of the water inhibitor is explored by monitoring the monomer conversion while the relative saturation of the nitrogen atmosphere is changed from 100% relative saturation to dry conditions. In this experiment, the thin film of vinyl ether monomer is illuminated for one minute while it is exposed to a nitrogen atmosphere of 100% relative saturation. The active centers produced during this time are quickly inhibited by reaction with water (Figure 7.1b), and no perceptible polymerization occurs (as shown in Figure 7.4). At the end of one minute, the lamp is shuttered off and the system is maintained in the dark, therefore no additional active centers are produced after the first minute. At a pre-

determined time (25 minutes), the water saturated nitrogen atmosphere was replaced with a dry nitrogen atmosphere while maintaining dark conditions. If the inhibition reaction shown in Figure 7.1b is reversible, the depletion of water by evaporation will move the equilibrium toward the left side of the reaction, and hydronium ions will be converted to free protons capable of initiating cationic polymerizations of the vinyl ether monomer.

Results for the experiment described above are shown in Figure 7.5. The figure illustrates that, as expected, no reaction is observed while the system is maintained in a nitrogen atmosphere of 100% relative saturation (during both the one minute of illumination and the subsequent 25 minutes in the dark). Therefore, any cations that exist in the system during this time are not active for cationic polymerization of the vinyl ether monomer. When the atmospheric conditions are changed to dry nitrogen, the figure illustrates that the polymerization is immediately observed even though the system continues to be maintained in the dark. Since all other conditions are constant, the observed polymerization must be a direct result of the changing atmospheric conditions, therefore the polymerization can be attributed to the evaporation of water. Figure 7.6 provides a more detailed view of the shape of the polymerization profile upon switching the atmosphere to dry nitrogen. The figure illustrates that a slow polymerization begins immediately after the dry nitrogen is introduced, and that after approximately 60 seconds, the polymerization rate accelerates considerably. The shape of this polymerization profile is influenced by the time for the water in the system to diffuse to the exposed surface, and subsequently evaporate into the atmosphere. All experimental observations are consistent with the conclusion that the inhibition reaction is reversible and that the active centers can be regenerated after remaining as unreactive hydronium ions for an extended period of time.

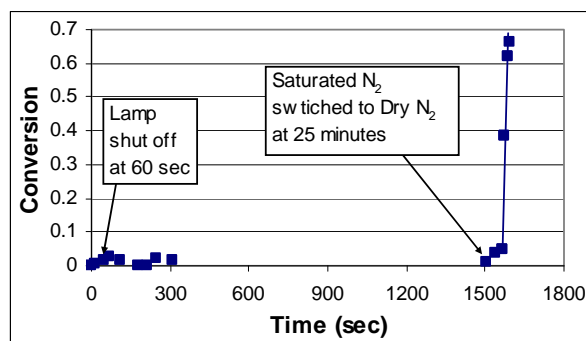


Figure 7.5. Monomer conversion vs. time for DVE under fully saturated nitrogen atmosphere which is switched to dry nitrogen atmospheric conditions after 25 minutes.

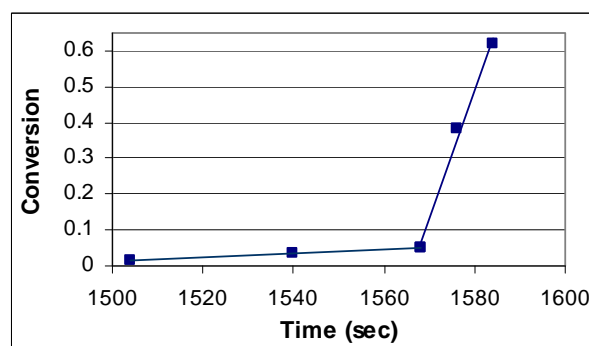


Figure 7.6. Monomer conversion of DVE vs. time immediately after a fully saturated nitrogen atmosphere is switched to dry nitrogen atmospheric conditions at 25 minutes.

7.5. Conclusion

This contribution further enhances knowledge of water inhibition in cationic photopolymerizations. For conditions of constant humidity in thin film systems, it was found the degree of inhibition increased with increasing humidity, and that a saturated atmosphere leads to complete inhibition. Furthermore, it was shown that a completely inhibited system can experience a rapid polymerization, even after 25 minutes in the dark, when the system is purged with dry nitrogen causing the water to evaporate and the inhibition reaction to be reversed.

These results illustrate the potential of vinyl ether cationic photopolymerization to be controlled temporally by the water concentration in the atmosphere.

CHAPTER 8: CONCLUSIONS AND RECOMMENDATIONS

This research has explored the unique characteristics of cationic active centers which allow cationic photopolymerization to be used in many new applications where previous photopolymerization techniques failed. Cationic active centers are essentially non-terminating which cause extremely long active center lifetimes. With these long lifetimes, the active centers were found to be very mobile allowing them to migrate into and polymerize regions that were never illuminated in a process termed as shadow cure. The ability to shadow cure allowed the cationic active centers to be used in the efficient polymerization of thick or pigmented systems where light attenuation had previously limited photopolymerization. The long lifetimes of the cationic active centers were used in the creation of a sequential stage curable polymer system and in the development of a novel method to cure complex shapes. The reversible termination of the cationic active centers was also examined and used as a technique for external temporal control of the photopolymerization after the illumination has ceased. An overview of major conclusions and future recommended research for each of these applications is provided.

8.1. Cationic Photopolymerization's Ability to Cure Thick Systems through Active Center Migration

The long lived cationic active centers were shown to be mobile and have the ability to cure thick polymer systems by migrating from the illuminated regions where they were created into deeper unilluminated regions of the thick sample. An analysis based upon the set of fundamental differential equations which govern the evolution of the light intensity gradient and initiator concentration gradient revealed that active centers are created only in the first few millimeters of a thick sample. Experimental results revealed that the active centers migrate from these first few millimeters into deeper regions up to a centimeter through reaction diffusion. The migration was shown to be proportional to the square root of time with effective shadow

cure diffusion coefficients consistent with a small molecule diffusing through a highly crosslinked network. Increases in temperature, propagation rate (via counter-ion size), active center concentration gradient, and total number of active centers (via exposure time) all increase the extent of shadow cure and exhibited higher effective shadow cure diffusion coefficients. The fundamental knowledge gained from this research provides the ability to design an efficient photopolymerization of thick polymer systems.

Photopolymerization of thick systems is an important emerging technology that could be significantly enhanced through the use of cationic shadow curing. While the fundamental characterization is complete, future work is recommended to further enhance the understanding of active center migration through thick systems. Research into how the degree of crosslinking in the monomer network affects active center migration is needed. These studies all were of a highly crosslinked network which severely impedes active center migration. Linear or low crosslinked network might exhibit an immense increase in active center migration. The structure and composition of monomer resins' influence on the active center migration could be characterized as well. Another important aspect to shadow curing that must be investigated is the property development of shadow cure. Whether the properties of the sample's shadow cure portion matches that of the regular photocure portion of the sample or if a property gradient is formed should be researched. With these studies, the active center migration process could be optimized and widespread applications implemented.

8.2. Cationic Photopolymerization's Ability to Cure Pigmented Systems

The mobility of long-lived cationic active centers was utilized to fully polymerize pigmented or filled systems overcoming the additive interference. Finite element analysis of the active center generation found the depths at which active centers are generated in a sample decreases by two to four orders of magnitude in the presence of the additive (from ~0.7mm to

less than a micron). Despite this reduction in active centers, experimental studies revealed that cationic photopolymerizations can efficiently polymerize pigmented systems by migrating beyond the depth of light penetration. Similar to shadow curing thick polymer systems without additives, it was found increasing the overall amount of active centers will increase the cationic active center migration speed and reduce the time it takes to fully cure a coating with additives. Very basic additives (such as HALS) were found to inhibit the cationic active center polymerization. These fundamental studies on cationic active center migration through pigmented systems have important implications in a variety of applications where pigments and fillers are necessary.

Pigments and weathering agents are only a small portion of the possible additives to polymer systems. Many other additives are available and need to be studied for their effects on cationic active center migration. Antifoaming agents, aluminum flakes, conductive particles, nanoparticles, expanding fillers, and surfactants are just a few types of additives that could be tested. Similarly, as with the thick systems, the properties of the shadow cure coatings as compared to thermo or dual coatings should be investigated.

8.3. Cationic Photopolymerization's Ability to Cure Complex Shapes

Cationic active centers were revealed to be especially long lived when created by illumination in monomer-free solutions. These solutions were shown to be stored up to six weeks without any loss of reactivity upon contact with the monomer. Storing the previously photogenerated active centers at temperatures up to 50°C also had no effect on their reactivity. These previously photogenerated active centers created by the illumination of photoinitiators in monomer-free solutions can be used to cure complex shapes by applying them as a second wet coating on a monomer coating substrate or by simultaneous applying them with the monomer

coating the complex substrate. Polymerizing complex shapes in this novel method will eliminate the typical problems of both the oxygen inhibition and shadow regions.

More research must be performed before this new method can be implemented. The process must be optimized. For example, finding the ideal previously photogenerated active center to monomer ratio must be investigated so no photoinitiator is wasted but a complete cure is obtained. In addition, the properties of coatings applied in this novel method must be studied to ensure comparable results to standard photo or thermopolymerizations. Once the optimization studies are completed, the process could be implemented photopolymerizing coatings on many different complex substrates such as automotive bodies, gears, or pipe fittings.

8.4. Creating Sequential Stage Curable Polymers with Cationic Photopolymerizations

Sequential stage curable systems (with three distinct stages) are only possible due to the cationic active center lifetimes being long enough to support length between the stages. The temporal control of the discrete stages in sequential stage curable material can be achieved through the composition of the monomer resin or by using a free radical/iodonium salt photoinitiator with the addition of an amine. Control through composition of the monomer was achieved by adjusting the concentration of the highly crosslinked acrylate network thus reducing the mobility of the cationic active center and delaying the start of the polymerization (establishment of the 3rd stage). The addition of an amine in a free radical/iodonium salt photoinitiator can also be used to temporally control the sequential stages by adjusting the basicity of the added amine. More basic amines will lengthen the time the system is in the second stage and delay the onset of the cationic polymerization/third stage. The temporal control and unique properties of the distinct stages make sequential, stage-curable hybrid photopolymerization systems attractive for a wide variety of applications.

Expanding the research of the sequential stage curable hybrid photopolymerization from kinetics into the properties of the individual stages would be very valuable. The properties of the individual stages need to be defined in order to design and implement a sequential stage curable hybrid system. Once the properties are defined, the system could be used for dental composites, microfluidics, or pressure sensitive adhesives.

8.5. Cationic Photopolymerizations Ability to Achieve Temporal Control of Polymerization Through a Reversible Water Inhibition

A technique for temporally controlling cationic photopolymerization after the illumination has ceased was developed for vinyl ethers that do not contain hydroxyl end groups. Through externally controlling the atmospheric moisture the vinyl ether polymerization can be inhibited and started at will once the active centers are created. In a saturated atmosphere the cationic active centers are completely inhibited. However, this inhibition is reversible. The polymerization can experience a rapid polymerization, even after 25 minutes in the dark, when the saturated atmosphere is purged. These results illustrate the potential of vinyl ether cationic photopolymerization to be controlled temporally by the water concentration in the atmosphere.

There is a great deal more research on this topic that needs to be performed. Investigations into the effects of several parameters such as photoinitiator type, concentration, and temperature need to be addressed. Also, research on whether the water inhibition can be reversed for other cationic monomers needs to be performed. If this reversible inhibition holds true for other monomers, then it could be applied in a wide variety of applications where temporal control after illumination is needed.

REFERENCES

1. Wicks Jr ZW, Jones FN, Pappas SP. Organic Coatings, 2nd ed., John Wiley & Son Inc., New York, NY 1994.
2. Weiss KD. *Paint and coatings: A mature industry in transition*. Prog. Polymer Sci., **1997**. 22: 203-245.
3. Decker C. *Photoinitiated crosslinking polymerisation* Prog. Polymer Sci., **1996**. 21: 593-650
4. Odian G. Principles of Polymerization, 3rd ed., John Wiley & Son Inc., New York, NY 1991.
5. Koleske JV. Radiation Curing of Coatings., ASTM International, West Conshohocken, PA 2002.
6. L Gou, B Opheim, AB Scranton. *Methods to Overcome oxygen inhibition in free radical photopolymerizations* in Photochemistry and UV Curing: New Trends. JP Fouassier Ed., Research Signpost, Kerala, India 2006. pp 300-310
7. Decker C. *Light-induced crosslinking polymerization* Polymer Int., **2002**. 51(11): 1141-1150
8. Decker C, Nguyen Thi Viet T, Decker D, Weber-Koehl E, *UV-radiation curing of acrylate/epoxide systems* Polymer, **2001**. 42(13): 5531-5541
9. Decker C, *Photoinitiated curing of multifunctional monomers* Acta Polymer., **1994**. 45(5): 333-347
10. Lin Y, Stansbury J, *The impact of water on photopolymerization kinetics of methacrylate/vinyl ether hybrid system* Polym. Adv. Technol., 2005. 16: 195-199
11. Mecerreyes D, Pomposo JA, Bengoetxea M, Grande H, *Novel Pyrrole End-Functional Macromonomers Prepared by Ring-Opening and Atom-Transfer Radical Polymerizations* Macromolecules, **2000**. 33(16): 5846-5849
12. Itoh H, Kameyama A, Nihikubo T, *Synthesis of new hybrid monomers and oligomers containing cationic and radical polymerizable vinyl groups and their photoinitiated polymerization* J. Polym. Sci. Part A: Polym. Chem., **1996**. 34(2): 217-225
13. Degirmenci M, Hepuzer Y, Yagci Y, *One-step, one-pot photoinitiation of free radical and free radical promoted cationic polymerizations* J. App. Polym. Sci., **2002**. 85(11): 2389-2395

14. Baikerikar KK, Scranton AB, *Photopolymerizable liquid encapsulants for microelectronic devices* Polymer, **2001**. 42(2): 431-441
15. Baikerikar KK, Scranton AB, *Photopolymerizable liquid encapsulants for microelectronic devices: Thermal and mechanical properties of systems with reduced in-mold cure times* J. Appl. Polym. Sci., **2001**. 81(14): 3449-3461
16. Stephenson N, Kriks D, El-Maazawi M, Scranton AB, *Spatial and temporal evolution of the photo initiation rate for thick polymer systems illuminated on both sides* Polymer Inter., **2005**. 54(10): 1429-1439
17. Mills P, *Robotic UV Curing for Automotive Exterior Applications*. Radtech Report, **2005**. July/August 2005: 23-30
18. Decker C, Moussa K, *Real-time kinetic study of laser-induced polymerization* Macromolecules, **1989**. 22: 4455-4462
19. Takahashi, E, Sanda F, Endo T, *Photocationic and radical polymerizations of epoxides and acrylates by novel sulfonium salts* J. Polym. Sci. Part A: Polym. Chem., **2003**. 41(23): 3816-3827
20. Rehm D, Weller A, *Kinetics of fluorescence quenching by electron and H-atom transfer* Isr. J. Chem., **1970**. 8: 259-271
21. Oxman JD, Jacobs DW, Trom MC, Sipani V, Ficek B, Scranton AB, *Evaluation of initiator systems for controlled and sequentially curable free-radical/cationic hybrid photopolymerizations* J. Polym. Sci. Part A: Polym. Chem., **2005**. 43(9): 1747-1756
22. Decker C, Moussa K, *Kinetic study of the cationic photopolymerization of epoxy monomers* J. Polym. Sci. Part A: Polym. Chem., **1990**. 28(12): 3429-3443
23. Crivello JV, *The discovery of and Development of Onium Salt Cationic Photoinitiators* J. Polym. Sci. Part A: Polym. Chem., **1999**. 37(23): 4241-4254
24. Smith GH, *U.S. Patent 4,394,403* **1983**.
Belgium Patent 828,841 **1975**.
25. Crivello JV, *U.S. Patent 3,981,8987* **1976**.
26. Jang M, CrivelloJV, *Synthesis and cationic photopolymerization of epoxy-functional siloxane monomers and oligomers* J. Polym. Sci. Part A: Polym. Chem., **2003**. 41(19): 3056-3073

27. Sasaki H, Rudzinski JM, Kakuchi T, *Photoinitiated cationic polymerization of oxetane formulated with oxirane* J. Polym. Sci. Part A: Polym. Chem., 1995. 33(11): 1807-1816
28. Decker C, presented at the 2005 Fundamental of Photopolymerizations Conference, Breckenridge, Co, June **2005**.
29. Decker C, Le Xuan H, Nguyen Thi Viet T, *Photocrosslinking of functionalized rubber. III. Polymerization of multifunctional monomers in epoxidized liquid natural rubber* J. Polym. Sci. Part A: Polym. Chem., **1996**. 34(9), 1771-1781
30. Sipani V, Scranton AB, *Kinetic studies of cationic photopolymerizations of phenyl glycidyl ether: termination/trapping rate constants for iodonium photoinitiators* J. Photochem. Photobio. A: Chem., **2003**. 159(2): 189-195
31. Sipani V, Scranton AB, *Dark-cure studies of cationic photopolymerizations of epoxides: Characterization of the active center lifetime and kinetic rate constants* J. Polym. Sci. Part A: Polym. Chem., **2003**. 41(13): 2064-2072
32. Hull CW, *U.S. Patent 4,575,330* **1986**.
33. Keaveney T, *Cationic UV technology and its applications in the coatings industry*. Ink and Print, **1995**. Sept. 22 1995: 1-6
34. Roth JD, *U.S. Patent 5,889,084* **1999**.
35. Kenning NS, Kirks D, El-Maazawi M, Scranton AB, *Spatial and temporal evolution of the photoinitiation rate for thick polymer systems illuminated with polychromatic light* Polym. Int., **2006**. 55(9): 994-1008
36. Cussler EL, *Diffusion: Mass Transfer in Fluid Systems*, Cambridge University Press, New York, NY 1984.
37. Anseth KS, Wang CM, Bowman CN, *A Photochromic Technique To Study Polymer Network Volume Distributions and Microstructure during Photopolymerizations* Macromolecules **1994**. 27(10): 650-655
38. Anseth KS, Kline LM, Walker TA, Anderson KJ, Bowman CN, *Reaction Kinetics and Volume Relaxation during Polymerizations of Multiethylene Glycol Dimethacrylates* Macromolecules, **1995**. 28(7): 2491-2499
39. Nelson EW, Jacobs JL, Scranton AB, Anseth KS, Bowman CN, *Photo-differential scanning calorimetry studies of cationic polymerizations of divinyl ethers* Polymer, **1995**. 36(24): 4651-4656

40. Nelson EW, Scranton AB, *Kinetics of cationic photopolymerizations of divinyl ethers characterized using in situ Raman spectroscopy* . Polym. Sci. Part A: Polym. Chem., **1996**. 34(3): 403-411
41. Dean K, Cook WD, *Effect of Curing Sequence on the Photopolymerization and Thermal Curing Kinetics of Dimethacrylate/Epoxy Interpenetrating Polymer Networks* Macromolecules, **2002**. 35(21): 7942-7954
42. Dean K, Cook WD, Rey L, Galy J, Sautereau H, *Near-Infrared and Rheological Investigations of Epoxy-Vinyl Ester Interpenetrating Polymer Networks* Macromolecules **2001**. 34(19): 6623-6630
43. Dean K, Cook WD, Zipper MD, Burchill P, *Curing behaviour of IPNs formed from model VERs and epoxy systems I amine cured epoxy* Polymer **2001**. 42(4): 1345-1359
44. Lin Y, Stansbury JW, *Kinetics studies of hybrid structure formation by controlled photopolymerization* Polymer **2003**. 44(17): 4781-4789
45. Oxman JD, Trom MC, Jacobs DW, *US Patent 6,187,836* **2001**.
46. Oxman JD, Jacobs DW, *US Patent 6,025,406* **2000**.
47. Lin Y, Stansbury JW, *Near-infrared spectroscopy investigation of water effects on the cationic photopolymerization of vinyl ether systems* J. Polym. Sci. Part A: Polym. Chem., **2004**. **42(8)**: 1985-1998
48. Crivello JV, Falk B, Zonca Jr. MR, *Study of cationic ring-opening photopolymerizations using optical pyrometry* J. App. Poly. Sci., **2004**. 92(5):3303-3319
49. Sangermano M, Malucelli G, Morel F, Decker C, Priola A, *Cationic photopolymerization of vinyl ether systems: influence of the presence of hydrogen donor additives* Europ. Poly. J., **1999**. 35(4): 639-645
50. Hartwig A, Schneider B, Luhring A, *Influence of moisture on the photochemically induced polymerisation of epoxy groups in different chemical environment* Polymer, **2002**. 43(15): 4243-4250